Abstract

Natural killer (NK) cells destroy virus-infected and tumor cells without prior antigen stimulation. The NK cell cytotoxicity is regulated largely by the expression of NK cell receptors that are able to bind major histocompatibility complex (MHC) class I glycoproteins. NK cells also express lysis triggering receptors specific for non-MHC ligands, including NKp30, NKp44, NKp46 and CD16. However, the nature of their ligands, recognized on target cells, is undefined. The activating receptors play a key role in activating the NK cells by specifically binding the activating ligands. The study conducted here deals with finding out activating ligands from tumor antigen database. It employs a computational approach to determine the binding pattern of NKp30 complexed with ligand B7H6 [PDB ID=3PV6] and finding out structural homologue of the ligand from tumor antigen database (T-Antigen Database). The homologues obtained were then subjected to molecular docking using HADDOCK web server. The ligand complexed with NKp30 showing lowest binding energy (energetically favorable) was simulated using Molecular Dynamics simulations to determine its stability in dynamic bodily conditions. The study also deals with finding the binding site of hemagglutinnin with NKp44 and NKp46. Experimental studies have already proven hemagglutinnin to be the activating ligand of NKp44 and NKp46 but due to lack of information of the binding site involved, further studies have been restricted. The study also presents the structural aspect of HLA-G and KIR2Dl4 interaction and the comparison of the binding affinity of KIR2DL4 with other class I HLA molecules- HLA-E, HLA-Cw3 and HLA-Cw4. The reliability of experimental procedure employed here has been validated by showing higher binding affinity of KIR2DL4 with HLA-G and lower binding efficiency with HLA-E, as reported by some previous studies. Residues of KIR2DL4, important for interactions, have also been explored. The study also revealed a greater binding efficiency of HLA-Cw3 and Cw4 with KIR2DL4, suggesting some unexplored role of KIR2DL4.

Chapter-1

Objective – To identify new activating ligands for NKp30 and to deduce the structural basis of NKp44 and NKp46 interaction with its known ligand hemagglutinin.

1. Introduction

Natural Killer (NK) cells are large granular lymphocytes of the innate immune system. They do not require prior sensitization with an antigen and play important role in host defense by killing broad range of virus-infected and tumor transformed cells. NK cytotoxicity is regulated by a fine balance between activation and inhibition signals by a multitude of receptors stochastically expressed on each NK cell. Structural studies have revealed that many inhibiting NK cell receptors recognize major histocompatibility complex (MHC) class I proteins and tumor antigens with varying degrees of peptide specificity. Killer cell immunoglobulin-like receptor (KIR) genes regulates NK cell function, which varies substantially between individuals in their number and type. Thus, specific inherited KIR-HLA combinations in different individuals have variable susceptibility to infection and cancer. The distribution of these receptors in NK cells in different organs varies, leading to different levels of NK activity. Structural basis for this variation in NK activity has not yet been explored. In order to design better immune therapeutic strategies for cancer treatment, we need to explore the structural basis of the different inhibitory receptor with their ligands and how the expression level of receptors is altered in NK cells in different organs. Further very limited structural information is available about the activating receptors and their cognate ligands. Putative tumor expressed ligands for activating NK receptors have been investigated which will help to design novel strategies for NK and CTL potentiation and help design novel therapeutic strategies.

It has been seen that interaction of NK cell receptors with non classical MHC molecules (HLA-G, E) is involved in suppression of NK cell activity against trophoblast cells in uterus. We have also shown greater inhibition of non classical MHC molecules with NKG2A as opposed to classical MHC binding KIRs (Das and Long, 2010). A better understanding about the binding mode and the important residues involved in interactions is needed for exploring the structural basis for NK receptor mediated inhibition by non-classical MHC molecules. This may further be correlated to the predisposition of certain MHC haplotype. Activation of NK cell plays a very important part in immunological response. Studies have been carried out to identify ligands for certain NK cell receptors but the co-expression of multitude of activating and inhibitory receptors on NK cells has made such studies difficult. A computational NK activating receptor driven exploration of ligands and their systematic investigation in tumor antigen pool will help fishing out naturally occurring ligands for NK cell activation that may help device new therapeutic strategies for cancer.

2. Review of Literature

2.1 INTERNATIONAL STATUS

The biological activity of NK cells is controlled by a complex repertoire of surface receptors which upon engagement by ligands on a target cell signal either an inhibitory or activating response. Alteration in the expression of NK cell receptors changes the outcome of NK target interactions. It has been shown that the virus infected cells or tumor cells have been found to alter expression of inhibitory and activating receptors. A very recent study indicated that the distinct alteration of activating and inhibitory receptors expression on NK cells and its subsets occurred during HIV progression (Jiang Y *et al*. 2011). Patients with HHV8 viral infection have shown down-modulated expression of NKp30, NKp46 and CD161 receptors associated with impaired NK-cell cytotoxicity against target cells (Stephanie *et al*., 2012). Attempts have been made to investigate how ITIM receptor signaling impinges on activating pathways. It has been seen that the inhibitory form has intracellular ITIM, while the activating forms contain a positive transmembrane charged residue which facilitates interaction and signaling through the ITAM-containing DAP12 molecule (Joyce *et.al.* 2012). The possibility that autologous NK cells could serve as an effective treatment modality for solid tumors and viral infection has long been considered. Golden-Mason *et al.,* 2010 demonstrated a significant role of NK receptor (NKp30) in providing innate protection from Hepatitis C virus infection (HCV) in high risk individuals. It has been also shown that expansion of NK cells, from PBMC (peripheral mononuclear cells) and GMP compliant cell fractions derived by elutriation, shifted the NK cell receptor repertoire towards activation and resulted in cytotoxicity against various allogeneic tumor cell lines and autologous gastric cancer cells, while sparing normal PBMC with expanded NK cells mediating ADCC in an autologous and allogeneic setting by antibodies that are currently being used to treat patients with select solid tumors (Voskens *et al.* 2010). Studies reported during the last decade have shown that the roles of NK cells are not restricted to a killing function. For example, although decidual NK cells (dNK) cells are in close contact with fetal-derived trophoblasts at the fetal-maternal interface yet they are not cytotoxic against them. This could be the result of inhibitory interactions between the non-classical class I MHC molecules (HLA-E and HLA-G) and inhibitory receptors (KIR2DL4) on dNK cells (Manaster and Mandelboim, 2010). Role of activating KIR receptors in embryo implantation and the initial stages of pregnancy has been illuminated by Moffett and coworkers (S. E. Hiby *et al.* 2010). Their studies indicate that the presence of the activating KIR2DS1 receptor may influence embryo implantation and prevent reproductive failure. It has been investigated that phenotypic evolutions of decidual NK cells may preserve NK cell activation/inhibition balance during the first trimester of pregnancy. It has also been shown that the expression of CD85J, NKG2D, NKp30, NKp44, KIR2DL1/S1 and KIR2DL2/L3/S2 receptors at the cell surface evolves between 8 and 12 weeks of gestation (Marlin *et al.* 2012). Thus there is a temporal NK regulation but induced receptor expression. However further studies are required for complete elucidation of NK receptor mediated regulation of NK tumor cytotoxicity.

2.2 NATIONAL STATUS

Killer cell immunoglobulin-like receptors (KIR) regulate natural killer cell response against infection and malignancy. Individual differences in NK-cell interactions and response to infections are dependent on the combinations of variable killer immunoglobulin-like receptor (KIR) and HLA class-I gene products. Interaction between KIR and HLA- B allele, HLA-B*40 and HLA-B*08 is associated with the risk of breast cancer (Gopalkrishnan *et al.* 2006). Also, unusual receptor-ligand interactions may result in altered NK-cell-mediated immunity. It has been proposed that altered KIR-HLA-C interaction results in over-activation of activating genes that may contribute to disorders such as recurrent miscarriage (Faridi and Aggarwal, 2011). Studies have been carried out to identify KIR genes distribution and their association with tuberculosis. It has been also reported that inhibitory genes KIR3DL1, KIR2DL3 and activating genes KIR2DS1, KIR2DS5 are involved in susceptibility towards *Mycobacterium tuberculosis* either individually or in haplotype combinations (Pydi *et al.* 2012). Clinical outcome of KIR-ligand mis-match interaction on graft-versus-host disease has also been observed (Kanga *et al.* 2012). There is need to examine influence of HLA genotypes on risk of cancer. But the knowledge about KIR-ligand interaction and their influence on the cancer is scarce. So, it is important to determine the binding affinity of the receptors with different allelic forms of MHC molecules and their influence on the risk of cancer.

2.3 Natural Cytotoxicity Receptors

The natural cytotoxicity receptors have been identified as the effector molecules responsible for the majority of NK driven cytotoxicity against tumor cells or virally infected cells, with blocking of these receptors resulting in significantly decreased NK cell killing (A. Moretta *et al.,* 2001). The NCRs are made up of three Ig-like proteins named NKp46, NKp30, and NKp44. NKp46 and NKp30 are constitutively expressed on NK cells while NKp44 is expressed upon IL-2 driven activation of NK cells. To date, all three proteins have been structurally characterized (Figure 1) but some controversy still surrounds their ligands due to the absence of ligand bound structure

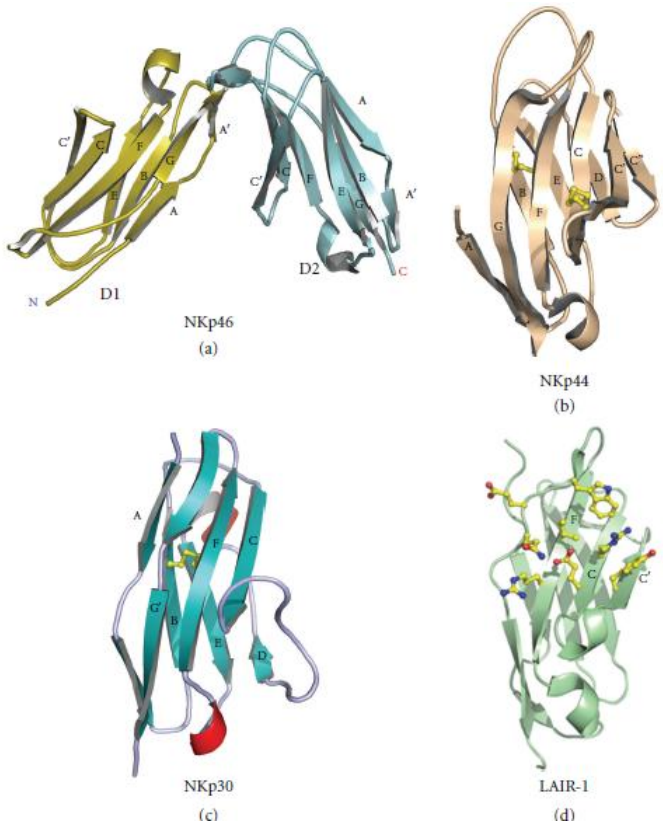

Figure 1 : Stucture of Natural Cytotoxicity receptors in cartoon representation a) NKp46 b) NKp30 c) NKp44 d) structure of LAIR-1 with collagen binding residues shown in ball and stick representation. (Courtesy: Joyce and Sun, 2011)

Structure	Resolution (Å)	PDB ID	Reference
NKp46	2.2	1P6F	Foster *et al.*
NKp46	1.9	1OLL	Ponassi *et al.*
NKp44	2.2	1HKF	Cantoni *et al.*
NKp30	1.8	3NOI	Joyce *et al.*

Table no. 1: Showing the structures of Natural Cytotoxicity Receptors available with their resolutions, PDB ID and references.

2.3.1 NKp46

NKp46 was first identified by Moretta and coworkers in 1997 as a cell surface receptor expressed on freshly isolated and activated NK cells and plays a pivotal role in natural cytotoxicity and targeting of transformed cells (S. Sivori *et al.* 1997). NKp46 is critical to NK cell activation in response to Newcastle disease virus (M. Jarahian *et.al* 2009), primary tumor melanocytes (E. Cagnano *et al.* 2009), urothelial cancers (V. Yutkin *et al.*,2007), medulloblastoma (R. Castriconi *et al.*, 2007), myeloma cancer (Y. M. El-Sherbiny *et. al*, 2007), filovirus infected dendritic cells (C. L. Fuller *et al.*, 2007), Herpes simplex virus (S. E. Chisholm *et al.* ,2007), vaccinia virus (S. E. Chisholm *et al.* ,2007), influenza virus, parainfluenza and sendai viruses (O. Mandelboim *et al*.,2007), and the response to *Mycobacterium tuberculosis* infected monocytes (A. Garg, P. F. Barnes *et al.* , 2007). NKp46 is a type I membrane protein made up of two N-terminal Ig-like extracellular domains, a 40 amino acid linker region, single transmembrane domain and a short highly charged 25 amino acid cytoplasmic region. NKp46 contains three glycosylation sites, two of which are located in the 40 amino acid stalk region and one in the D2 domain at Thr 225. NKp46 lacks an activating cytoplasmic component but through a transmembrane Arg residue associates with CD3ζ and FcεRIγ which can transmit a cell activating signal via their multiple ITAM containing domains. A number of viral hemagglutinin, neuraminidase-hemagglutinin proteins which become surface expressed following viral infection have been proposed as ligands. In addition, Vimentin binding by NKp46 following mycobacteria infection of monocytes has been described (A. Garg, P. F. Barnes *et al.*, 2007). NKp46 binding of specific heparan sulfate proteoglycans has also been proposed as a ligand and may be critical for tumor cell killing but its relevance to virally infected cell killing is unclear (M. L. Hecht *et al.*, 2007; A. Zilka *et al.*, 2007).

The structure of NKp46 was determined by X-ray crystallography in 2003 (C. E. Foster *et al.*, 2003; M. Ponassi *et al.*, 2003*)* revealing a structure made up of two C2-type Ig-like domains (Figure 2). Each domain is made up of eight β-strands which form two β-sheets with a typical disulphide bond formed between each sheet maintaining the Ig-domain fold. The two domains are maintained at an angle of 85° respective to each other by a large number of hydrophobic interactions and extensive hydrogen bonding. An area of 1021 Å is buried between the two NKp46 domains illustrating the extensive interactions and within the core region of the domain interactions, 11 of 18 amino acids are conserved in NKp46 sequences from diverse species. Although associated by function with NKp30 and NKp44, NKp46 shows very low homology to the other natural cytotoxicity receptors (Figure 1). The most structurally similar molecules to NKp46 include the KIR family of proteins, ILT2 ((B. E. Willcox *et al*., 2003) RMSD: 2.2 Å, hinge angle: 86°), glycoprotein VI ((K. Horii *et al.*, 2006) RMSD: 1.6 Å, hinge angle: 90°) and also FcαRI ((A. B. Herr *et al*., 2003) CD89; RMSD: 2.4 Å; hinge angle: 92°). All these molecules have a very similar overall fold made up of two C2 type Ig-like domains and a hinge angle comparable to that observed in NKp46 (Figure 2). Altogether, the description of the binding sites of these homologous proteins suggests that NKp46 would also utilize the hinge region for ligand binding and the

description of a ligand binding site as determined from structural studies or large-scale mutagenesis is eagerly anticipated.

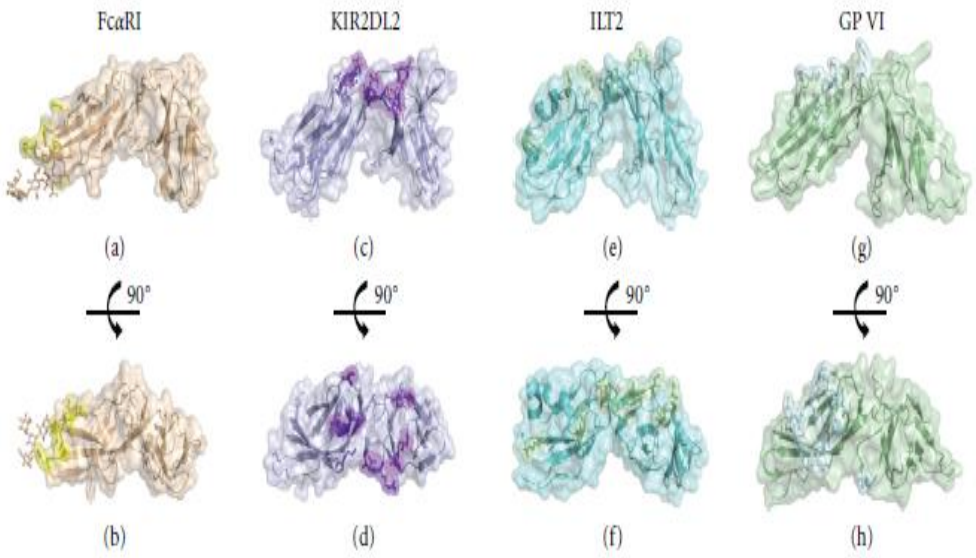

Figure 2: Structures of NKp46 homologous proteins ((a), (b)) Fc*α*RI, ((c), (d)) KIR2DL2, ((e), (f)) ILT2 and ((g), (h)) GP VI shown in cartoon representation with transparent surface also shown. The known ligand binding residues of these molecules are given in ball and stick representation with the surface of these amino acids also highlighted. KIR binding to MHC molecules utilizes a number of residues found in the AB, CC*'*, EF loop regions of D1, the GA hinge region between D1 and D2, and the BC loop and FG loop regions of D2. ILT-2 uses residues located in the C strand, the CE loop region, EF loop region, and G strand of D1 while also using residues located in the BC loop region of D2. GP VI utilizes residues in the CC*'* loop, C strand, CE loop, E strand, EF loop and F strand of D1 while also using the FG loop region of D2. CD89 uses residues from the BC loop, C*'* strand, C*'*E loop, and the FG loop of D1 in a side-on mechanism of binding in contrast to the other homologous proteins which all utilize the membrane distal face of the receptor for ligand binding. The lower panel shows the respective molecules in an "above-cell view" orientation which also highlights their ligand binding sites (Courtesy: Joyce and Sun 2011).

2.3.2 NKp44

NKp44 is a natural cytotoxicity receptor which is found on activated NK cells and leads to enhanced killing of both tumor cells and virally infected cells (T. I. Arnon *et al.*, 2001, C. Cantoni et. al ,1999, M. Vitale et. al.1998). NKp44 is made up of a single extracellular IgV domain with a 64 amino acid stalk region which contains a number of glycosylation sites, a transmembrane region containing a lys residue, and a short cytoplasmic domain. Following NKp44 ligand binding, NK cell activation signals are transduced via DAP12 which associates with NKp44 through its transmembrane domain. The crystal structure of the extracellular domain of NKp44 displays a compact V domain structure (C. Cantoni *et al.*, 2003). It is made up of two typical *β*-sheets constructing the Ig-V domain structure. Unique features of this structure include the presence of a second disulphide bond which in combination with the atypical orientation of the equivalent CDR3 loop region creates a large grooved area on one face of the protein. This groove is also positively charged and has been proposed as a ligand binding site. The NKp44 structure is homologous to a number of other Ig-like structures

including TREM-1 (triggering receptor expressed on myeloid cells; RMSD: 2.0 Å) (M. S. Kelker *et al*. 2004, S. Radaev *et al.* 2003), TREM-like transcript-1 (RMSD: 1.7 Å) (J. L. Gattis *et al.* 2006), poly Ig receptor (RMSD: 2.1 Å) (A. E. Hamburger et. al 2004.), sialoadhesin (RMSD: 2.4 Å) (N. R. Zaccai *et al.* 2007) and IREM-1 (inhibitory receptor expressed on myeloid cells, RMSD: 2.58 Å) (J. A. Marquez *et al.* 2007) (Figure 3).

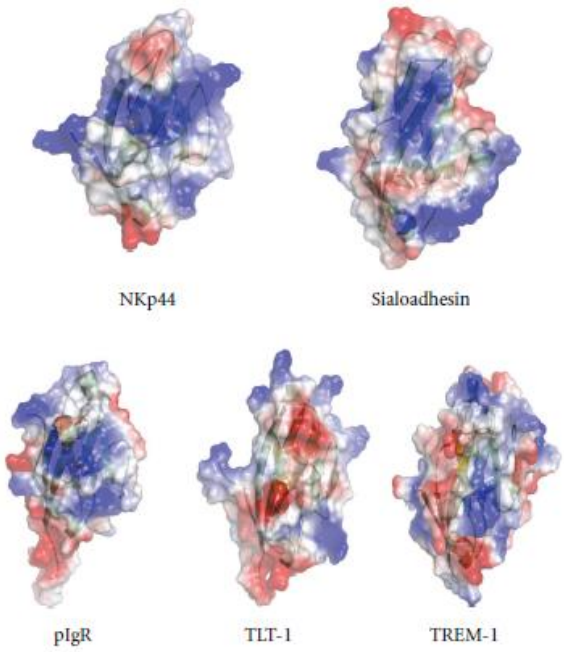

Figure 3: Charged surface representation of NKp44 and closely related homologues sialoadhesin, pIgR, TLT-1 and TREM-1.

2.3.3 NKp30

The most recently discovered NCR is NKp30 which was identified by Moretta and coworkers (D. Pende *et al.* 1999). NKp30 has been shown to be the dominant activating receptor responsible for the lysis of a number of tumor cell types (D. Pende *et al.* 1999). In addition, NKp30 has been shown to cause the activation and expansion of resting NK cells upon interaction with DCs and to cause the death of imDCs (G. Ferlazzo *et al.* 2002). NKp30 has a single extracellular Ig-like domain with a short stalk region (5 amino acids), and a transmembrane domain which associates with CD3ζ homodimers through a charged transmembrane interaction. The physiological ligands for NKp30 remain a controversial issue as a large number of NKp30 interacting molecules have been proposed. These include a human cytomegalovirus tegument protein pp65 (T. I. Arnon *et al.* 2005), duffy-binding-like-(DBL-) 1α of *Plasmodium falciparum* erythrocyte membrane protein- 1 (*Pf* EMP-1) (E. Mavoungou *et al.* ,2007), leukocyte antigen-B-associated transcript 3 (BAT3) (E. Pogge von Strandmann *et al.*,2007, V. R. Simhadri *et.al.* 2008,) and a group of heparan sulfate/heparin

molecules (M. L.Hecht *et.al.* 2009). Most recently, NKp30 was shown to recognize a B7 family homolog (B7-H6) as its ligand (C. S. Brandt *et al.* 2009). Unlike the other protein ligands proposed, B7-H6 is expressed on a number of tumor cell lines, such as K562 and Raji, as well as on primary cancer cells. However, the lack of structural information for NKp30 makes it difficult to parse out the most important ligand involved in cancer destruction from those proposed. The structure of NKp30 was recently, determined within our group and is shown to be a single I-type Ig-like domain (M. G. Joyce *et al.* 2011).The structure displays strong structural similarity to the CD28 family of receptors. Mutagenesis work carried out on NKp30 and binding studies on the B7H6 ligand indicates that binding is very similar to that observed for PD-1/PD-L1 interactions and involves residues found on the upper portion of the F and C strands.

3. Materials and Methods

3.1 Receptor Preparation

The structures of NK cell receptors were retrieved from RCSB PDB (Protein Data Bank). The structure of NKp30, NKp44 and NKp46 are available in PDB with PDB IDs 3PV6 , 1HKF, 1P6F respectively (Li, Y *et al.*,2011; Spallarossa, A *et al.*,2003; Foster, CE *et al.*,2003).The structures were prepared by deleting water molecules and all other hetero molecules (which were co crystallized). Viewerlite, molecular viewer by Accelerys, was used for carrying out the preparation of proteins. The prepared proteins were then subjected to energy minimization by pdb swissviewer which is a version of GROMOS 42B1 force field (Guex, N *et al.*,1997).The purpose of energy minimization is to prepare a protein by minimizing the net forces on atoms, hence bringing it to a stable molecular state.

3.2 Ligand Preparation

The ligand for NKp30 was obtained by deleting NKp30 from its co-crystallized structure. The structure of B7H6 thus obtained was minimized by pdb swissviewer. The structure of hemagglutinin having PDB ID 2VIU (Fleury *et al.*,1998) was retrieved from RCSB PDB. The bromelain digested chain of hemagglutinin, with a residue length of 328 amino acids, was chosen for studying interactions and was prepared in the same manner as B7H6.

3.3 Molecular Docking – HADDOCK Server

Protein–protein docking was performed using the Easy Interface docking protocol of Haddock Server (Sjoerd J. de Vries *et al.*,2007) which requires parameters like active residues and passive residues of the interacting proteins. Haddock (High Ambiguity Driven Protein-Protein Docking) is information driven flexible docking approach for modeling of biomolecular complexes. The approach adopted by the program is different from *ab-initio* docking protocols as it takes information from identified or predicted protein interfaces in ambiguous interaction restraints (AIRs) to drive the docking process (Dominguez C *et al.*,2003). The program makes use of the already existing experimental and bioinformatics data to accomplish docking process (Van Dijk A.D *et al.*,2003). Easy Interface module of HADDOCK requires proteins to be submitted in .pdb format along with information about the active (directly involved in interactions) and passive residues (surrounding surface residues).

3.4 Setting reference - NKp30 docked with B7H6

For the purpose of finding new activating ligands for NKp30, docking program was used to set a reference score. This was done by examining the interacting residues of NKp30-B7H6

and then subjecting the two proteins to docking protocol. Active residues for both proteins were defined by studying the H-bond forming residues in the complex by Viwerlite, while the passive residues were defined as the solvent accessible neighbors of active residue.

3.5 T-Antigen Database

The new activating ligand for NKp30 was identified from tumor antigen database, T-Antigen database. It is a data source and analysis platform for cancer vaccine target discovery focusing on human tumor antigens that contain HLA ligands and T cell epitopes. It contains 4,006 curated antigen entries representing 251 unique proteins. The database also provides information on T cell epitopes and HLA ligands with full references, gene expression profiles, antigen isoforms, and mutations (Developed by Bioinformatics Core at Cancer Vaccine Center, Dana-Farber Cancer Institute). Sequence of B7H6 was retrieved from PDB and given as a query for BLAST .The e value for the BLAST was set as .0001 to obtain best possible results and for the rest, default parameters were taken such as word size of 3, matrix to be used as BLOSSUM62 and gap costs as extension 11: extension 1. The results obtained were analyzed and the sequences of the homologue tumor antigen were retrieved from T-Antigen database. The user interface of T-Antigen Database is shown in figure 4.

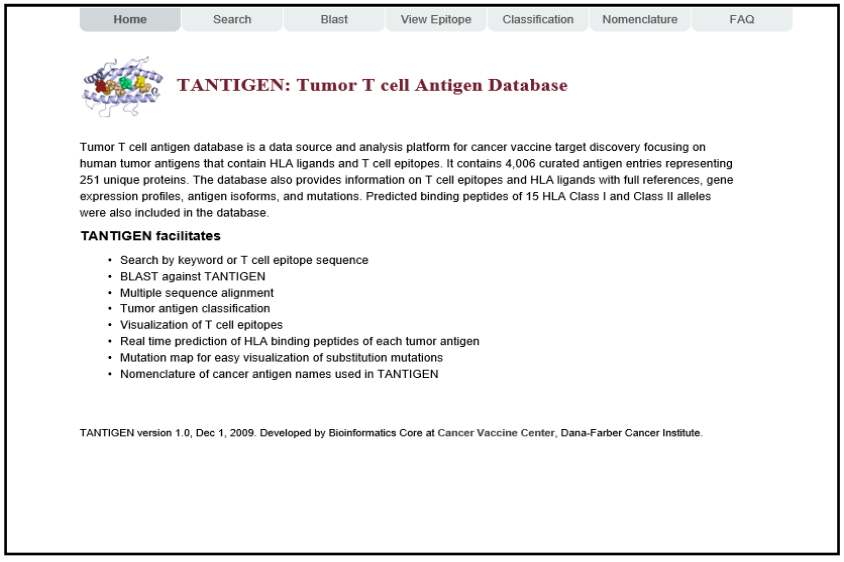

Figure 4: User Interface of T-Antigen Database.

3.6 Modeling of homologue hits

The hits obtained after local alignment of B7H6 with the sequences of tumor antigen were modeled with the aid of hybrid modeling server named Phyre2 (Soding, J. ,2005). Intensive modeling module was used for modeling the structures as it incorporates *ab-initio* folding simulation called Poing[2] to model the regions of proteins with no detectable homology to the known structures (B.R. Jefferys *et al.*,2010). Figure 5 shows the user interface of Phyre2.

Minimization of the modeled structures was followed by structural comparison to the ligand (B7H6) by PDB's Calculate Structural Alignment tool. The RMSDs obtained were recorded and structures showing larger deviation were discarded.

Figure 5: User interface of Phyre2

3.7 Docking of tumor antigens with NKp30 and deduction of their structural basis

The modeled structures with close structural similarity with B7H6 were docked with NKp30 by submitting the structures to HADDOCK Easy Interface server. The residues of NKp30 involved in interaction with B7H6 were selected as active residues and passive residues were taken as solvent accessible neighbors of those active residues. The active residues for the modeled structures were defined by examining the locally aligned stretches of modeled structures and B7H6 residues (which are involved in interaction with NKp30). The passive residues for the modeled structures were defined in a manner similar to that for NKp30.

3.8 Site of Docking for NKp44 and NKp46

For deduction of the site of interaction of NKp44 and NKp46, sequence alignment of both the receptor was done with NKp30 (whose site of interaction is known). The identical region found from the alignment was then compared with the site of interaction of the NKp30. The

finding was further matched with the cited literature to confirm it as the site of docking for NKp44 and NKp46.

3.9 Site of Docking for Hemagglutinin

For determining the site of interaction of hemagglutinin with NKp44 and NKp46, the structure of hemagglutinin was divided into 4 compartments covering the entire accessible area of the protein. The accessible area of the protein was determined by a program named ASAP (Accessible Surface Area Predictor) (http://ccb.imb.uq.edu.au/ASAP/) .The Easy Interface Docking protocol was used to dock hemagglutinin with both the receptors, taking the residues of each compartment one by one as active residues for it. The score for all the 8 procedures (four for each receptor) were taken into consideration and the score for the best compartment of active residues was analyzed for interaction studies.

3.10 Molecular Dynamic Simulations of the best Complexes

The complex of hemagglutinin with NKp44 and NKp46 having the lowest HADDOCK score (as lower score indicates greater binding efficiency) were subjected to MD run of 3000 ps each to determine the dynamic stability of the complexes by mimicking the *in-vivo* conditions. Desmond Molecular Dynamic System with Optimized Potential for Liquid Simulations (Jorgensen *et.al.*,1996 ;Kaminski *et al.*,2001) all atom force field was used to study the dynamic stability of the modeled protein. The missing residues were manually fixed. H-bonds were optimized by using H-bond assignment. The prepared complex was solvated in a triclinic periodic box of SPC water and then neutralized with appropriate number of counter-ions. The distance between the wall of the box and the complex was kept at 10 Å to prevent the interaction with its own periodic image. The prepared system was then subjected to energy minimization upto a maximum of 3000 steps using a steepest decent method or until a gradient threshold (25kcal/mol/Å) was reached. The equilibrated system was used to carry out further MD simulations for 3000 ps at a constant temperature of 300K and constant pressure of 1atm with a time step of 2fs. Smooth particle Mesh Edwald method was used to calculate long distance electrostatic interactions. A 9 Å cutoff radius was used for coloumbic short range interaction cutoff-method. Frames of the trajectory were captured every 4.8ps of the time interval.

4. Results and Discussion

4.1 Proposed new activating ligand of NKp30

4.1.1 Reference score of NKp30-B7H6

The HADDOCK Easy Interface docking protocol gave results for docking of NKp30-B7H6 in the form of 2 clusters having 175 structures. These were obtained from a three step protocol involving an initial stage of rigid docking to generate 1000 structures, followed by semi-flexible simulated annealing in torsion angle space of 200 best structures in terms of intermolecular energy (sum of Van der Waals, electrostatic and ambiguous interaction restraints energy terms). Final stage of the docking protocol involves inclusion of water in calculations to improve the energy of the structures. Clustering was done using a 3.5 Å RMSD cut-off and ranked according to their average interaction energies (sum of Electrostatic, van der Waal and Desolvation energy) and their average buried surface area according to the HADDOCK protocol. Out of these 2 clusters, the one with the lowest HADDOCK score was chosen and from that cluster the best structure was selected for further interaction analysis. Table no. 2 shows that the HADDOCK score for the best cluster was -52.2 +/- 2.0 .The cluster had 171 structures and the RMSD value from the lowest energy structure came out to be 0.7 +/- 0.5 Å. The statistical parameter, Z score was also calculated for the cluster which indicates how many standard deviations from the average this cluster is located in terms of score, which was observed to be high (Z= -1.0).

HADDOCK score	-52.2 +/- 2.0
Cluster size	171
RMSD from the overall lowest-energy structure	0.7 +/- 0.5
Van der Waals energy	-42.1 +/- 2.7
Electrostatic energy	-173.4 +/- 17.4
Desolvation energy	23.7 +/- 6.0
Restraints violation energy	9.5 +/- 11.84
Buried Surface Area	1325.6 +/- 39.8
Z-Score	-1.0

Table no. 2: HADDOCK score of top cluster of NKp30-B7H6 complex

The HADDOCK server also returns a graphical representation of clustering, done on various parameters including graphs of HADDOCK score v/s interface ligand RMSD, ligand RMSD

and Van Der Waal v/s liagnd RMSD. One of the graphs significant for analysis of the clustering is HADDOCK v/s i-l-RMSD graph as it provides information about the structure of lowest HADDOCK score. Figure 6 shows HADDOCK score in atomic units (a.u.) and RMSD in Å and the cluster with lowest energy shown in red.

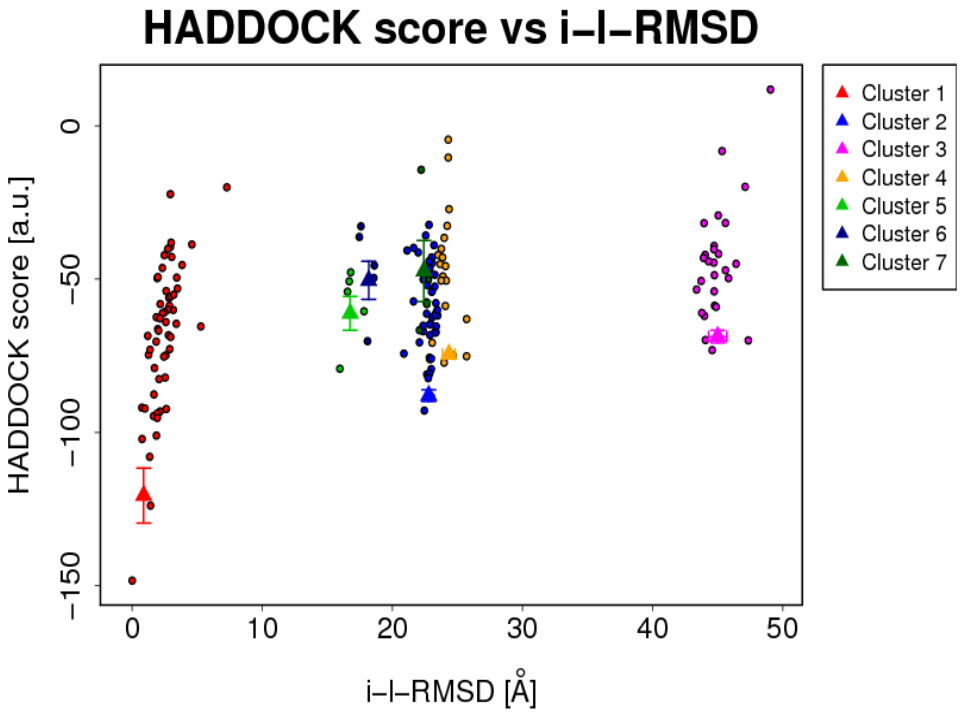

Figure 6: HADDOCK score v/s i-l-RMSD clustering graph for NKp30-B7H6

4.1.2 Homologues of B7H6 and their Structural similarity.

The sequence of B7H6 was submitted for BLAST search in T-Antigen database. Top seven hits, selected from the result shown in table no. 3, were used for further structural alignment with B7H6. The sequences of these hits were retrieved from T-Antigen database. These were used to model the protein structures with the aid of Phyre2 and finally subjected to structural alignment in order to rule out any structurally odd tumor antigen. All 5 modeled structures of tumor antigen showed a close resemblance in structure as the RMSD calculated ranged from 2.7 to 3.2 Å.

S. No.	Tumor Antigen ID	Score Bits	e value	RMSD(Å)
1.	Ag002094_TAPBP	41.2	$2e^{-05}$	3.04
2.	Ag000469_TAPB	41.2	$2e^{-05}$	2.78
3.	Ag002096_TAPBP	40.8	$2e^{-05}$	2.75
4.	Ag002095_TAPBP	40.8	$2e^{-05}$	2.78
5.	Ag002093_TAPBP	40.8	$3e^{-05}$	2.89
6.	Ag000467_TAPBP	40.4	$3e^{-05}$	3.10
7.	Ag000468_TAPBP	40.0	$4e^{-05}$	2.73

Table no. 3: BLAST result of B7H6 sequence with tumor antigen sequences.

4.1.3 Docking and interaction studies

All the structures showing high sequence and structural similarity with B7H6, were docked with NKp30. HADDOCK returns result in the form of clusters in which structures are clustered according to the HADDOCK score. The structure with the lowest HADDOCK score was considered for studying interactions as lower HADDOCK score reflects stronger binding (Dominguez C *et al.*,2003). Out of all the structures, antigen Ag_002094_TAPBP gave the highest HADDOCK score of -120.6 +/- 17.9 for a cluster having 56 structures (Table no. 4). From the cluster the best structure was chosen and further used for interaction analysis. The interaction analysis was done to identify that whether the new ligand was showing the same interaction pattern as NKp30-B7H6 complex

S.No	Statistic	Value
1	HADDOCK score	-120.6 +/- 17.9
2	Cluster size	56
3	RMSD from the overall lowest-energy structure	0.5 +/- 0.3
4	Van der Waals energy	-51.5 +/- 3.8
5	Electrostatic energy	-410.5 +/- 63.3
6	Desolvation energy	-2.1 +/- 12.1
7	Restraints violation energy	150.8 +/- 37.39
8	Buried Surface Area	2081.9 +/- 144.1
9	Z-Score	-2.0

Table no. 4: Statistics of the top cluster with highest energy among all other dockings

Interaction of NKp30 with Ag002094_TAPBP involving the same residues as in NKp30-B7H6 interaction provided sufficient evidence to propose the new ligand as activating ligand of NKp30. Figure 7 shows the clustering of complexes of NKp30 and Ag002094 on the basis of the HADDOCK score.

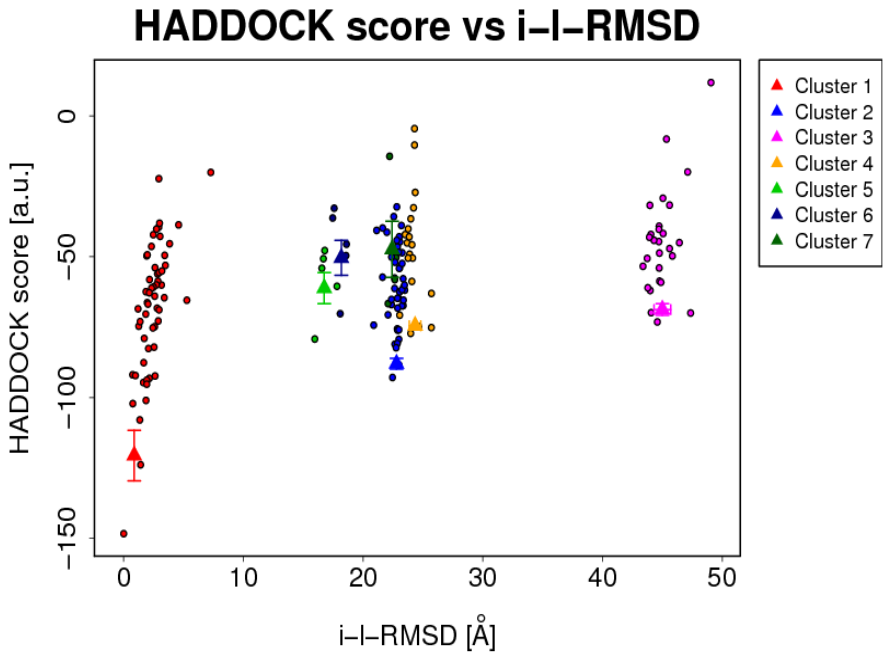

Figure 7: Clustering of structures obtained after docking of NKp30-Ag002904_TAPBP

The complex of NKp30 obtained after docking protocol was examined for H-bond forming residues. Table no. 5 shows that Val53, Glu65, Arg67, Asn68, Arg74, Ser 82, Arg96 and Glu111 are residues of NKp30 that were involved in H-bond interaction with the ligand B7H6. The length of the H- bonds was measured from Pymol. The H-bonding pattern of NKp30-B7H6 was then compared with NKp30-Ag002094_TAPBP (shown in Table no. 5 and Table no. 6). The comparison showed that the important residues of NKp30 interact with Ag002094_TAPBP in the same manner as our reference complex. Since NKp30 bound to Ag002094_TAPBP showed almost a similar interaction pattern as NKp30-B7H6, Ag_002094_TAPBP_TAPBP can be strongly proposed as a new activating ligand. Figure 8 and 9 shows the residues (highlighted in green) of NKp30-B7H6 and NKp30-Ag002094_TAPBP involved in H-bond interaction, respectively.

S.No	Residues involved in H bonds formation	
	B7H6 residues	NKp30 residues
1.	Asp 25	Arg74
2.	Leu26	Arg67
3.	Lys130	Glu111
4.	Thr127	Ser82
5.	Lys130	Arg67
6.	Asp25	Arg67
7.	Pro127	Val53

Table no. 5: Residues of B7H6 involved in H bonds formation with NKp30.

S.No	Residues involved in H bonds formation	
	Ag002094_TAPBP residues	NKp30 residues
1.	Thr127	Arg51
2.	Leu26	Arg67
3.	Lys130	Glu111
4.	Asp25	Arg74
5.	Lys130	Arg67
6.	Asp25	Arg67
7.	Pro128	Val53

Table no. 6: Residues of Ag002094_TAPBP involved in H bonds interaction with NKp30.

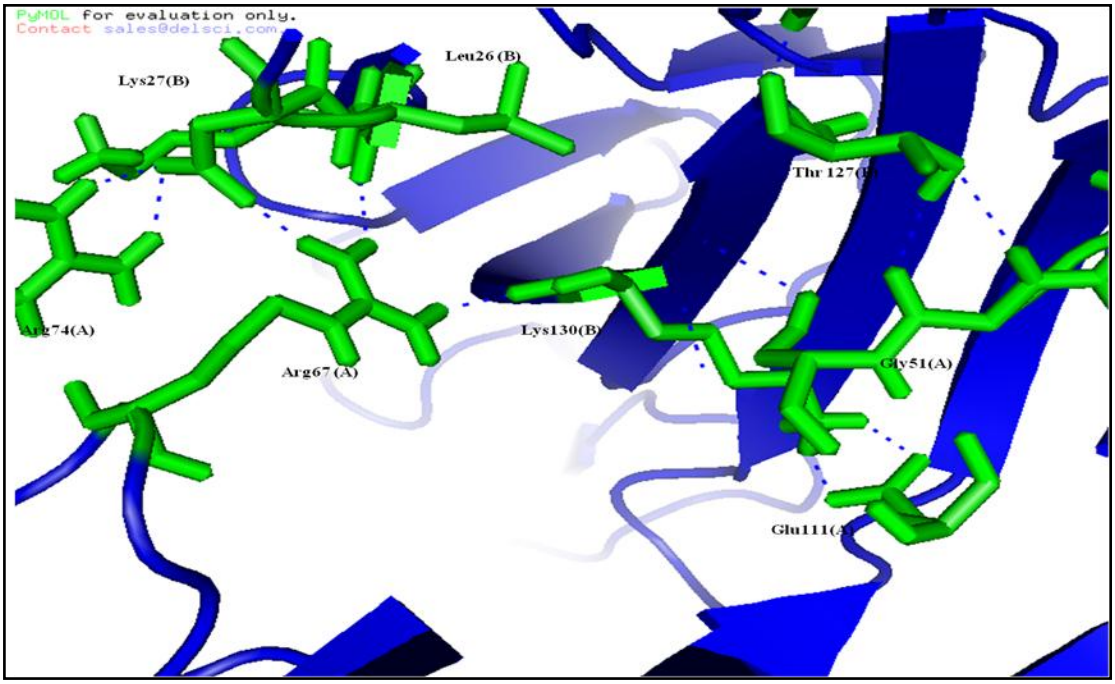

Figure 8: Shows the H-bond forming residues of NKp30-B7H6

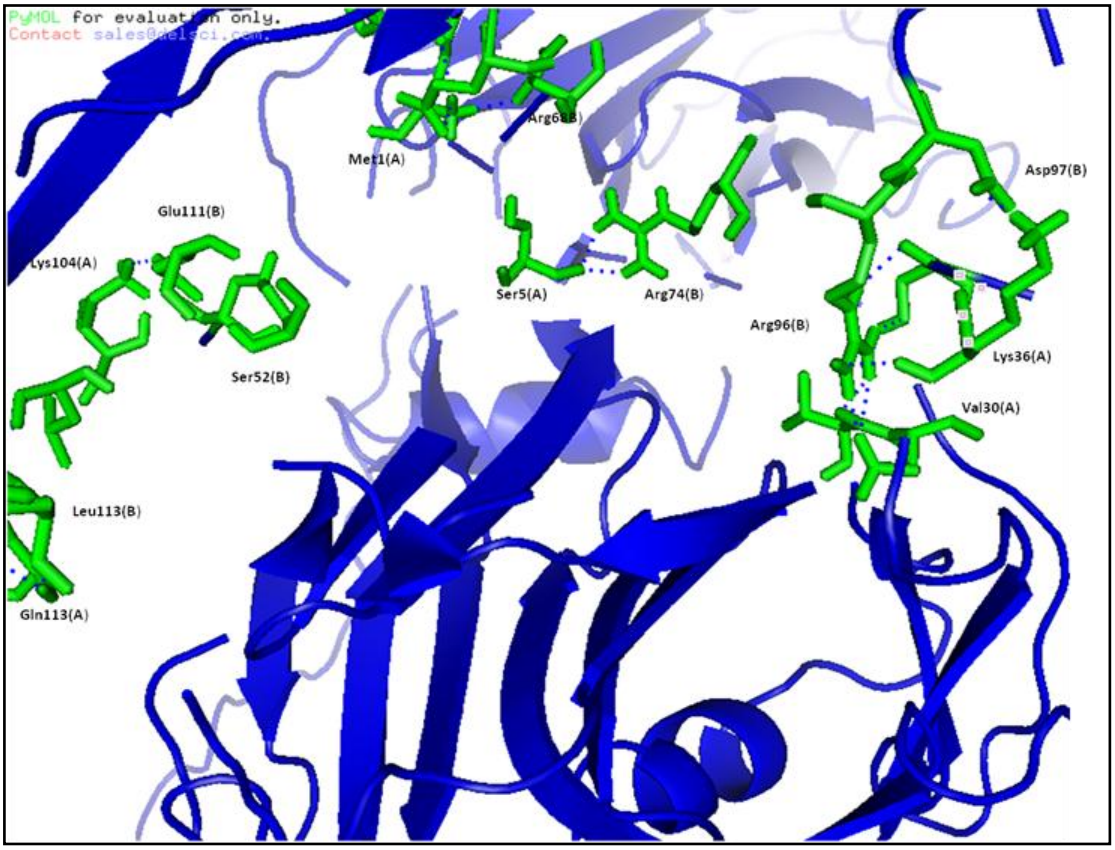

Figure 9: H-bond forming residues of NKp30-Ag002094_TAPBP

4.1.4 MD of NKp30-Ag002094_TAPBP Complex

Complex of NKp30-Ag002094_TAPBP was subjected to a simulation run of 3000ps.This was done in order to determine the stability of the complex in motion as molecular docking examines the interactions in static conditions only. Figure 10 shows the RMSD curve of the complex obtained after 3000 ps run. It shows that the complex deviated from its initial state but attained a stable posture at the end of the simulation. Since the complex was simulated in solvent molecules (SPC water) to mimic the *in-vivo* conditions, the interactions were examined again to identify the interacting residues which remained conserved during the simulation run. Average structure for the time frame of 1100ps to 2400ps was taken because of the relative complex stability in that time frame. It was found that almost all the H- bonds formed between the residues of Nkp30 and Ag002094_TAPBP were conserved. Table no. 7 shows the H- bonds conserved which remained conserved during the simulation run. Dynamically studying the complex further enforced the proposal of Ag002094_TAPBP as an activating ligand of NKp30. Figure 11 shows pre MD and post MD aligned structures. An RMSD of 0.138 Å was observed when the structures were aligned by pymol, suggesting a meager deviation in the structure of the complex even after 3000 ps .Figure 12 shows residues of NKp30-Ag002094_TAPBP involved in H-bond formation.

The new ligand shows 99% identity (79 % query coverage) with a structurally elucidated protein in PDB named tapasin with PDB ID= 3FU8 (Dong G *et al.* 2009). Tapasin is a glycoprotein, critical for loading major histocompatibility complex (MHC) class I molecules with high affinity peptides. It functions within the multimeric peptide loading complex (PLC) as a disulfide –linked, stable heterodimer with thethiol oxidoreductase ERp57. It has been shown that tapsin plays an important role in evading tumor progression. Jiang Q *et al.* in 2010 showed lack of expression of tapasin in tumors. The study conducted here discovers the ability of the new ligand (identical to Tapasin) to activate NKp30 by binding it in a similar fashion as B7H6. As shown by the previous studies (Jiang Q *et al.*,2010*)* the protein must be having some role to play in cancer epidemiology. With the results produced it can be proposed that tapasin has some role in activating NK cells and preventing tumor progression.

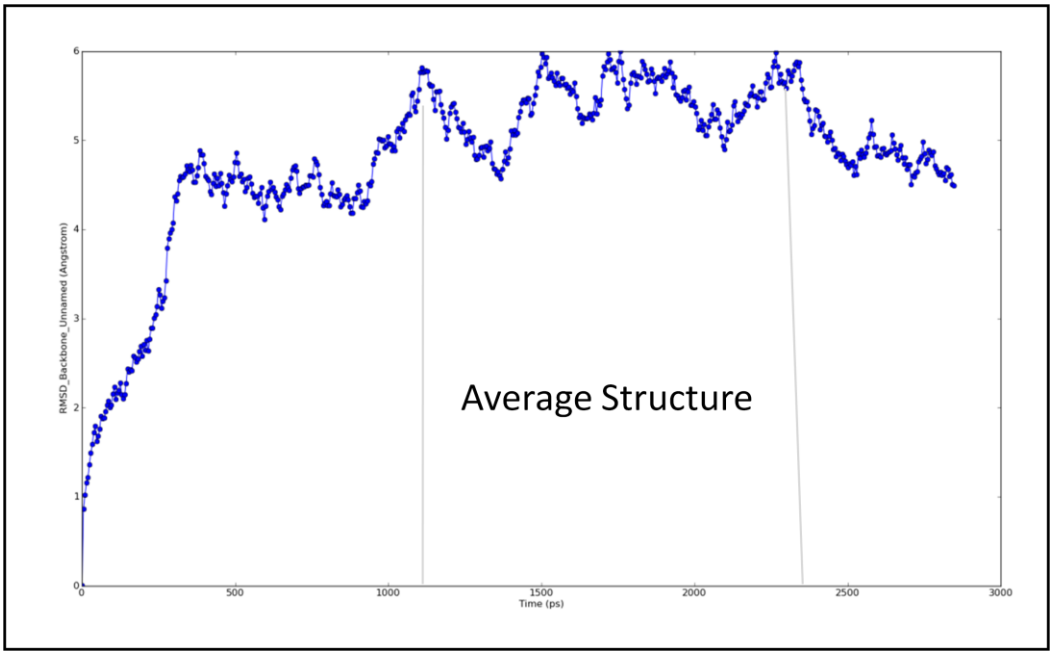

Figure 10: RMSD curve of NKp30-Ag002094_TAPBP with reference to initial structure after 3000ps of MD simulation run.

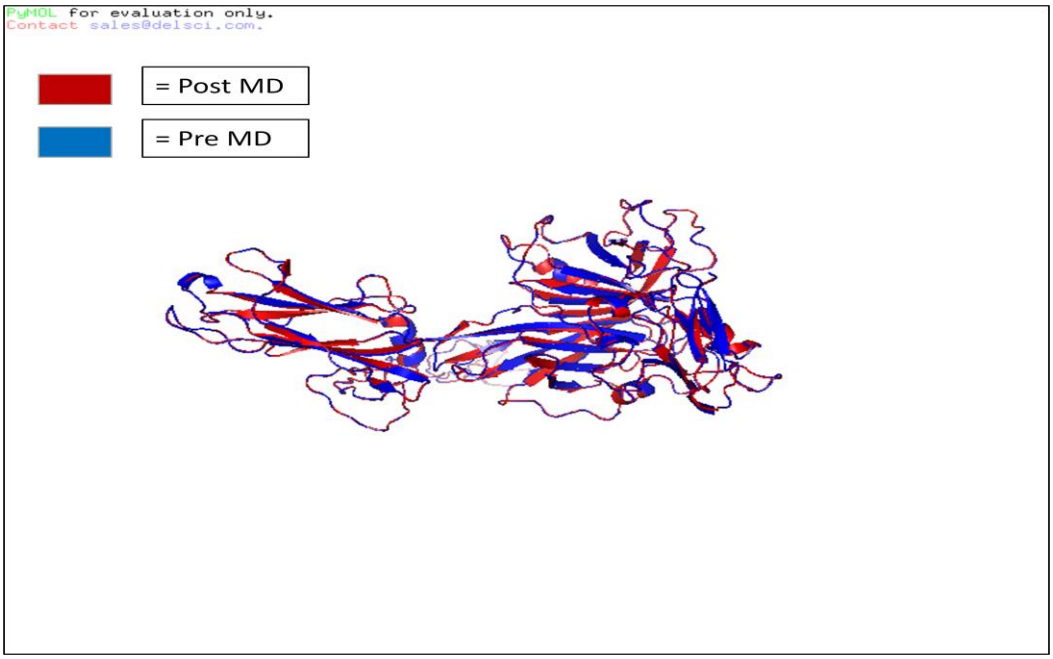

Figure 11: Alignment of NKp30-Ag002094_TAPBP before and after 3000ps simulation run.

S.No	Residues involved in H bonds after 3000ps simulation run	
	Ag_002094_TAPBP residues	NKp30 residues
1.	Asp 25	Arg74
2.	Leu26	Arg67
3.	Lys130	Glu111
4.	Thr127	Ser82
5.	Lys130	Arg67
6.	Asp25	Arg67
7.	Pro127	Val53

Table no. 7: Residues of Ag_002094_TAPBP involved in H bonds with NKp30 after 3000ps of simulation run.

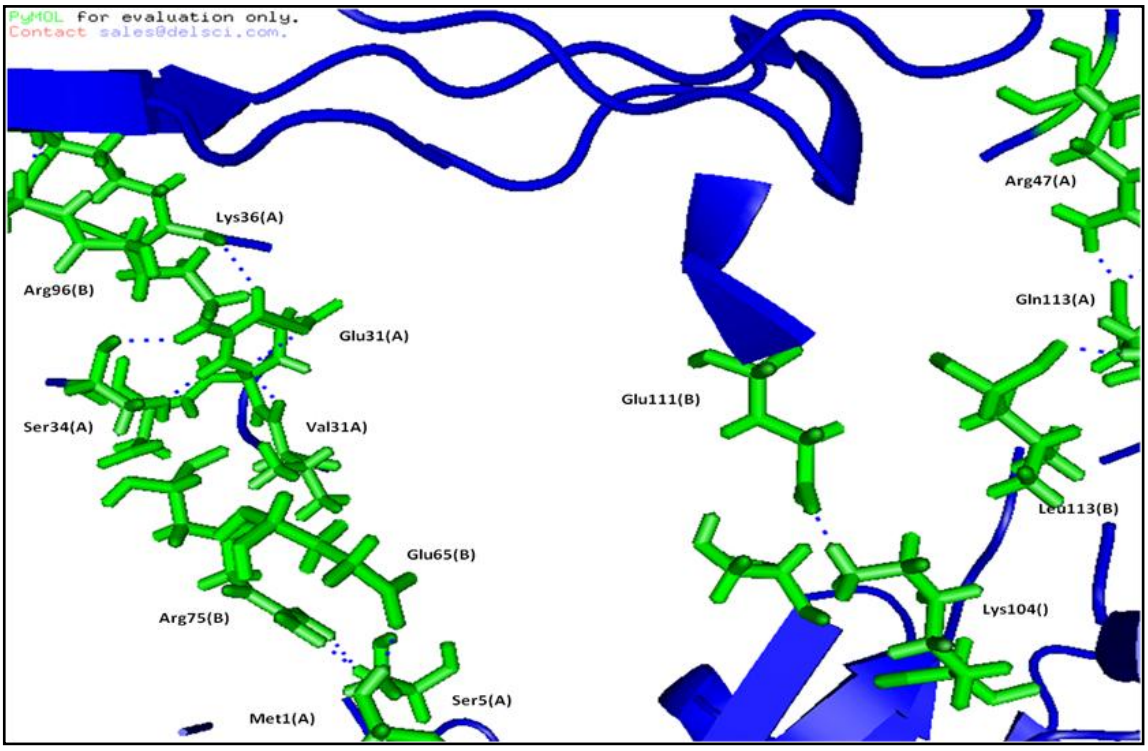

Figure 12: H-bond forming residues of NKp30-Ag_002094_TAPBP after 3000ps of simulation run.

4.2 Interaction studies of NKp46 and NKp44 with Hemagglutinin

4.2.1 HADDOCK results of NKp46-Hemagglutinin

The structure of hemagglutinin was divided into four compartments covering the entire solvent accessible area of the protein. The structure of hemagglutinin was analyzed for its surface accessible area by submitting its sequence to ASAP (Accessible Surface Area Predictor)(http://ccb.imb.uq.edu.au/ASAP/). The software takes a protein sequence in FASTA format. On the basis of the results obtained a compartment comprising of 12 residues was selected. These compartments were chosen on the basis of peaks representing higher accessible surface area of hemagglutinin (shown by figure 13). Each compartment was selected with residues showing high solvent accessibility. Table no. 8 shows the four compartments along with the residues which were considered active during the docking process. The results for docking process when the residues of each compartment were taken as the active residues of hemagglutinin are given in Table no. 8. The HADDOCK score for compartment 3 and 4 were almost the same. But for the purpose of interaction studies compartment 3 was chosen, because of the more negative Z score.

Compartment No.	Residues of compartment	HADDOCK score with NKp46	Z Score
1.	Glu119, Leu118, Phe120, Ile121,Thr122, Glu123, Phe125, Thr126, Trp127, Thr128, Gly129, Val130	-63.3+/- 20.1	-1.5
2.	Leu164, Asn165, Val166, Thr167, Met168, Pro169, Asn170, Asn171, Asp172, Asn173, Phe174, Asp175	-52.5 +/- 6.1	-1.4
3.	Tyr195, Val196, Glu197, Ala198, Ser199, Gly200, Arg201, Val202, Thr203, Val204, Ser205, Thr206	-81.3 +/- 3.3	-1.4
4.	Pro215, Asn216, Leu217, Gly218, Ser219, Arg220, Pro221, Trp222, Val223, Arg224, Gly225, Leu226	-81.3 +/- 3.3	-1.3

Table no. 8: shows the residues of the 4 compartments of hemagglutinin and their docking scores and Z scores with NKp46.

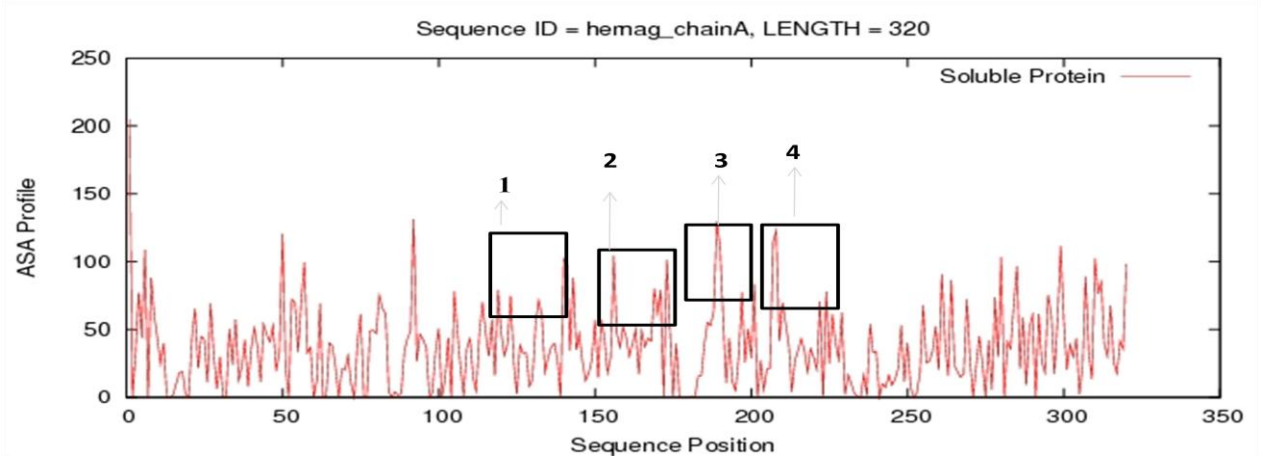

Figure 13: Result of ASAP and the regions of hemagglutinin protein selected as active site compartments.

5.2.1 H-bond interaction between hemagglutinin and NKp46

Complex of NKp46-hemagglutinin with active residues of hemagglutinin from compartment 3 was chosen for examining the H-bond interaction. Figure 14 shows that bonding pattern of the protein residues. Table no. 9 gives the list of the H-bond forming residues. The residues from the compartments 3 and 4 were involved in interactions with NKp30 which can be seen from docking scores. 8 strong H-bonds were found involved in stabilizing the complex.

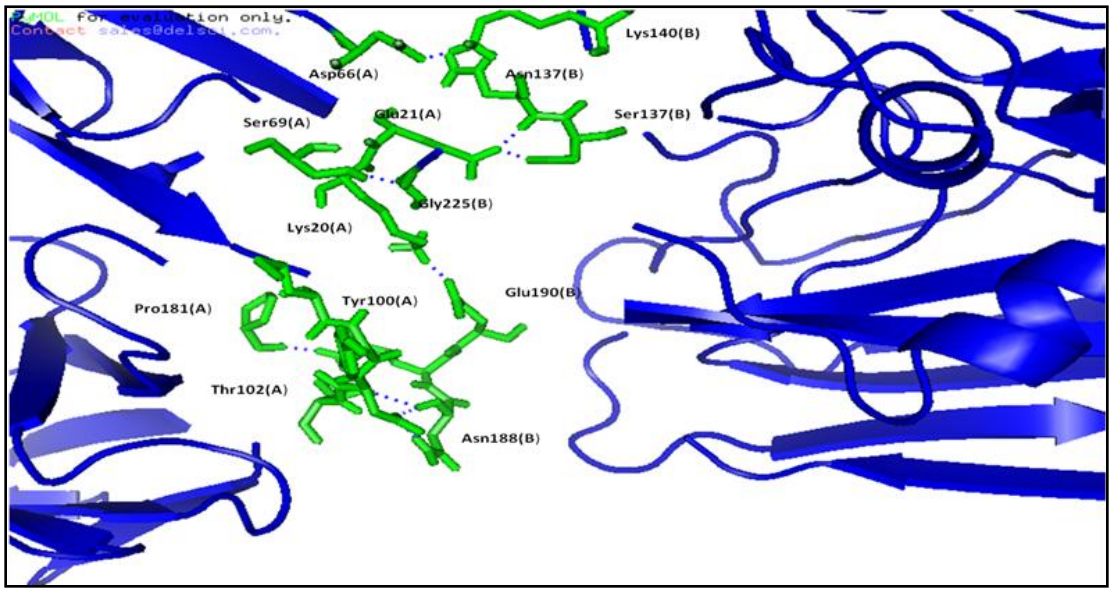

Figure 14: H-bond forming residues of NKp46-Hemagglutinin.

S.No	**Residues involved in H bonds**	
	Hemagglutinin residues	NKp46 residues
1.	Lys140	Asp66
2.	Ser136	Glu21
3.	Gly225	Ser69
4.	Ser228	Lys20
5.	Glu189	Pro180
6.	Tyr 105	Asp101
7.	Asn188	Asp101
8.	Pro128	Val53

Table no. 9: Residues of hemagglutinin involved in H bond formation with NKp46.

4.2.2 Molecular Dynamic Simulations of NKp46-hemagglutinin

After docking protocol the complex was subjected to molecular dynamics simulation run to determine the stability of the complex in bodily conditions. Desmond Molecular Dynamics System was used for simulating the complex for 3000ps. The docked complex obtained from molecular docking by Easy Interface HADDOCK protocol was first subjected to preprocessing. The missing residues were manually fixed. H-bonds were optimized by using H-bond assignment. The prepared complex was solvated in a triclinic periodic box of SPC water and then neutralized with appropriate number of counter-ions. The distance between the wall of the box and the complex was kept as 10 Å to prevent the interaction with its own periodic image. The prepared system was then subjected to energy minimization to a maximum of 3000 steps using a steepest decent method until a gradient threshold (25 kcal/mol/Å) was reached. The equilibrated system was then used to carry out further MD simulations for 3000 ps at a constant temperature of 300K and constant pressure of 1atm with a time step of 2 fs. Smooth particle Mesh Edwald method was used to calculate long distance electrostatic interactions. A 9 Å cutoff radius was used for coloumbic short range interaction cutoff-method. Frames of the trajectory were captured after every 4.8 ps of the time interval.

The RMSD curve obtained for NKp46-hemagglutinin complex showed deviation from 1 to 3 Å(shown by Figure 15). A stable trajectory of the complex was not obtained but the fluctuations experienced were not effective to change the interaction pattern as most of the H-bonds remained after 3000ps of simulation. The involvement of residues for H-bond formation was examined in the average structure of NKp46-hemagglutinin complex, computed for the time frame of 1200 to 2200 ps. The time frame was chosen for its stability as compared to the other time intervals. Figure 16 shows all the interacting residues of

NKp46 and hemagglutinin after 3000ps of simulations. Table no. 10 shows all the H bonds formed before simulation run were conserved except the bond between Lys 20 and Ser228.After 3000ps of run Lys formed a bond with Glu190.During an MD run the structure deviates from its initial state and the tries to attain the energetically favored conformation. Hence the slight change in the bonding pattern is a result of change acquired by the complex in mimicked *in-vivo* conditions.

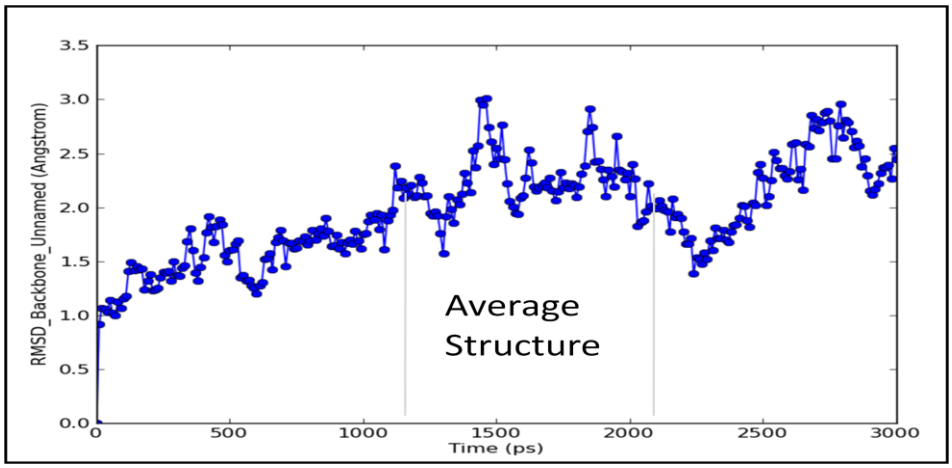

Figure 15: RMSD curve of complex NKp46-hemagglutinin for 3000ps simulation run

S.No	**Residues involved in H bonds**	
	Hemagglutinin residues	NKp46 residues
1.	Lys140	Asp66
2.	Ser136	Glu21
3.	Gly225	Ser69
4.	Ser228	Glu190
5.	Glu189	Pro181
6.	Tyr 105	Asp101
7.	Asn188	Asp101

Table no. 10: Residues involved in H bond interaction of NKp46-hemagglutinin after 3000ps of MD simulation run.

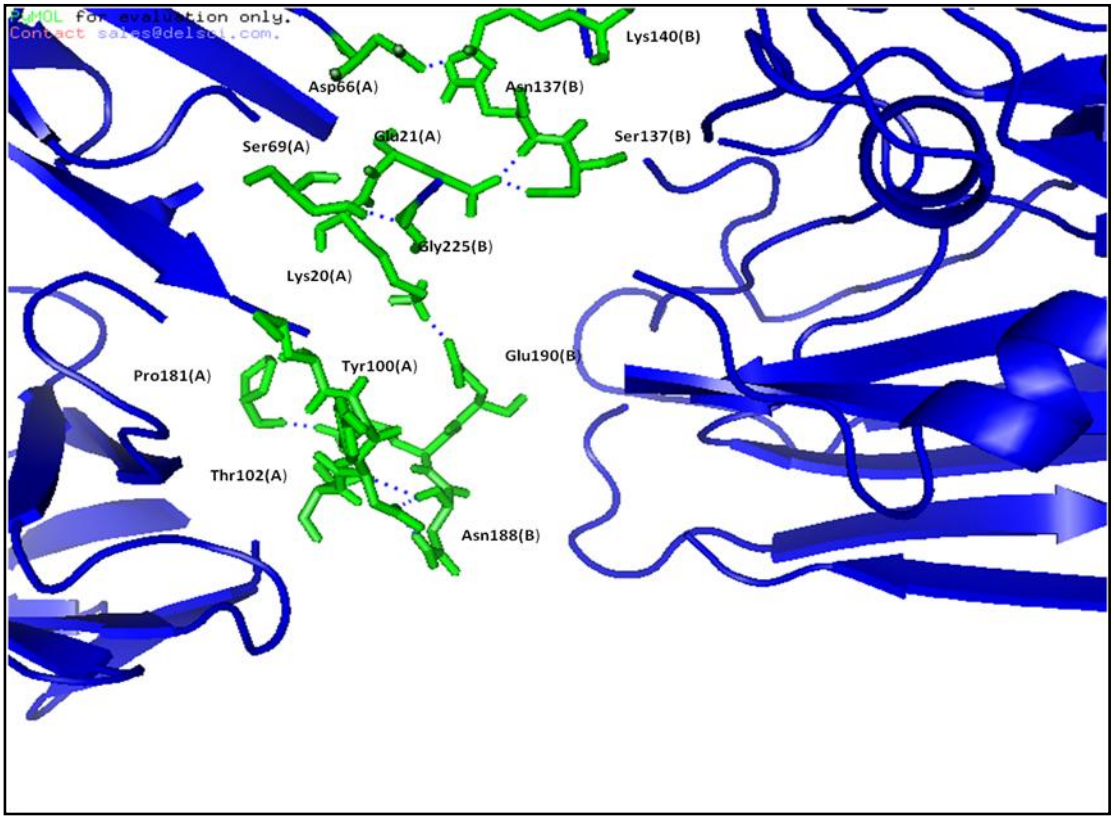

Figure 16: Residues of NKp46 and hemagglutinin involved in H bond formation after 3000ps simulation run

4.2.3 HADDOCK results of NKp44-Hemagglutinin

NKp44 was submitted along with hemagglutinin for HADDOCK docking protocol on HADDOCK Easy Interface web server. The active site for NKp44 was decided by aligning its sequence with NKp30 and NKp46. The identical residues found were then compared with the already known interacting site of NKp30. For hemagglutinin the same procedure was employed as in the case of docking with NKp46. Table no. 11 shows HADDOCK score of NKp44 and hemagglutinin when residues of different compartment were taken as active residues.

Compartment No.	Residues present in the compartment mentioned as active residues while docking	HADDOCK score with NKp44	Z Score
1.	Glu119,Leu118 ,Phe120,Ile121,Thr122,Glu123, Phe125,Thr126,Trp127,Thr128,Gly129,Val130	-60.8 +/- 6.1	-1.7
2.	Leu164,Asn165,Val166,Thr167,Met168,Pro169, Asn170,Asn171,Asp172,Asn173,Phe174 ,Asp175	-54.9 +/- 4.9	-1.6
3.	Tyr195,Val196,Glu197,Ala198,Ser199,Gly200,Arg 201,Val202 ,Thr203,Val204,Ser205,Thr206	-49.3 +/- 6.3	-2.3
4.	Pro215, Asn216, Leu217, Gly218, Ser219, Arg220, Pro221, Trp222, Val223, Arg224, Gly225, Leu226	-72.5+/-2.5	-1.9

Table no. 11: Residues of the 4 compartments of hemagglutinin and their HADDOCK and Z scores with NKp46

When the residues of compartment 4 were taken as active residues, lowest HADDOCK score was obtained, which indicated greater binding affinity (Dominguez C *et al.*,2003). The result reflected better binding of hemagglutinin with NKp44 when Pro215, Asn216, Leu217, Gly218, Ser219, Arg220, Pro221, Trp222, Val223, Arg224, Gly225 was taken as the residues of interacting surface of hemagglutinin. Figure 17 shows the H-bond interaction pattern between NKp44 and hemagglutinin.13 H bonds were observed in the docked complex. Table no. 12 shows the residues of Np44 and hemagglutinin, which formed H bonds.

S.No	**Residues involved in H bonds**	
	NKp44 residues	Hemagglutinin residues
1.	Lys33	Ile 217
2.	Ser 52	Asn216

3.	Lys33	Asn216
4.	Glu83	Lys299
5.	Ser112	Lys299
6.	Glu83	Arg269
7.	Glu84	Arg109
8.	Arg82	Ser110
9.	Arg62	Asp104
10.	Ser61	Asp104
11.	Arg47	Asp101
12.	Asp97	Ser219
13.	Asp98	Ser219

Table no. 12: Residues of NKp44 and hemagglutinin involved in H bond formation.

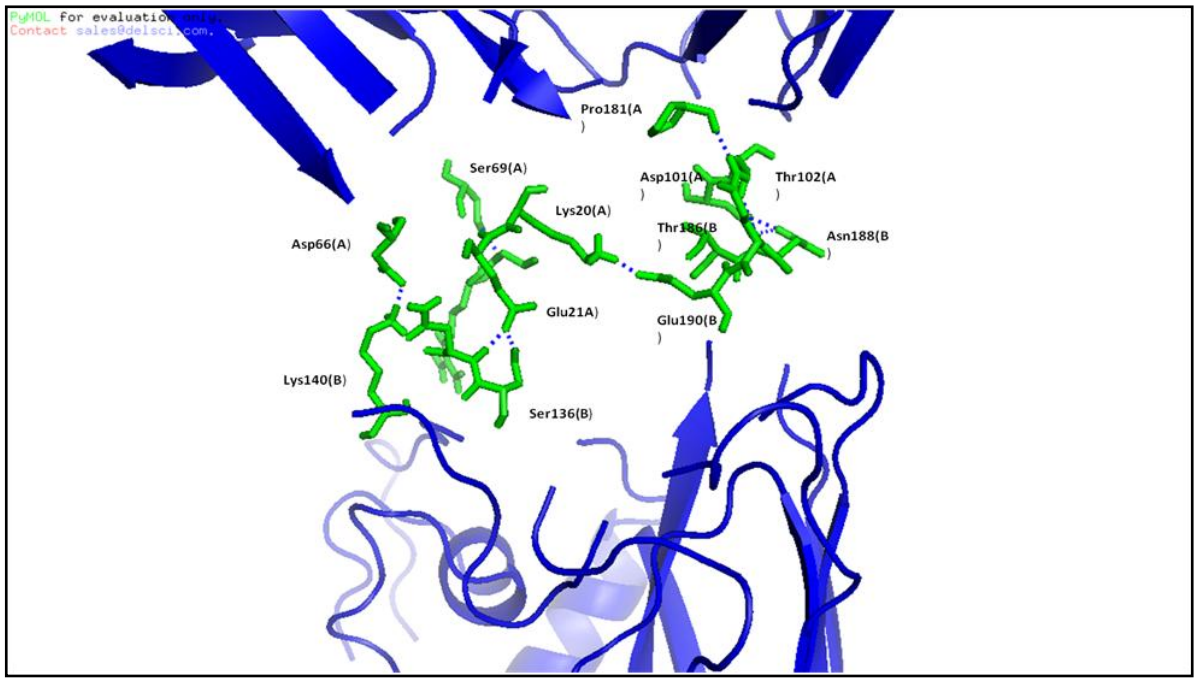

Figure 17: H-bond forming residues of NKp44-Hemagglutinin.

4.2.4 Molecular Dynamics Simulation of NKp44-hemagglutinin

The docked complex obtained after HADDOCK docking protocol need to studied dynamically as molecular docking studies the proteins in static conditions. In order to get a dynamic perspective the docked complex was subjected to 3000ps simulation run using Desmond Molecular Dynamics System. The missing residues were manually fixed. H-bonds were optimized by using H-bond assignment. The prepared complex was solvated in a triclinic periodic box of SPC water and then neutralized with appropriate number of counter-ions. The distance between the wall of the box and the complex was taken as 10 Å to prevent the interaction with its own periodic image. The prepared system was then subjected to energy minimization to a maximum of 3000 steps using a steepest decent method until a gradient threshold (25 kcal/mol/Å) was reached. The equilibrated system was used to carry out further MD Simulations for 3000 ps at a constant temperature of 300K and constant pressure of 1atm with a time step of 2fs. Smooth particle Mesh Edwald method was used to calculate long distance electrostatic interactions. A 9 Å cutoff radius was used for coloumbic short range interaction cutoff-method. Frames of the trajectory were captured every 4.8 ps of the time interval.

The RMSD curve (shown in figure 18) obtained showed deviation from 1 to 4 Å during the run. The structure initially deviated for a short period of time and after 600ps attained a stable trajectory which persisted till 2100 ps. After 2100 ps the structure deviatiation was again observed but acquired stability after 2700 ps. The structure remained very stable during the time frame of 600ps to 2000ps with only a few minor deviations. To study the interaction pattern after simulations an average structure was made by extracting frames of the simulations from 600 to 2000ps because of relative stability of the complex. This structure was then analyzed for H bond interaction pattern. Figure 19 shows the residues of NKp44-hemagglutinin participating in H-bond formation.

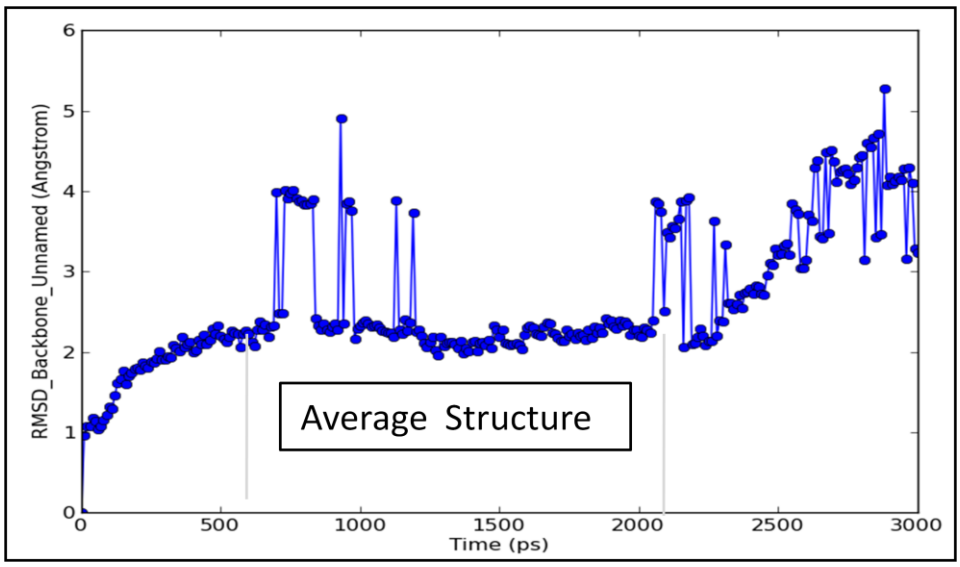

Figure 18: RMSD curve of complex NKp44-hemagglutinin for 3000ps simulation run.

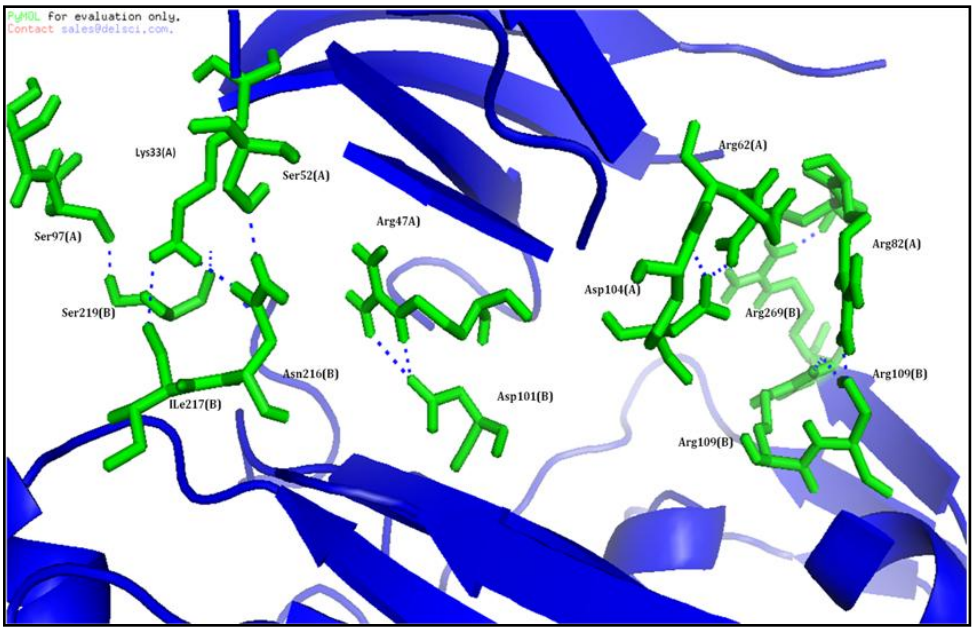

Figure 19: H-bond forming residues of NKp44-Hemagglutinin after 3000ps of simulation run.

The stability of the complex was determined by examining the residues involved in interactions after 3000ps. It was seen that 11 out of 13 residues retained their interactions with their binding partner. Some new H-bonds were also formed, resulting from residues moving close to each other during the simulation run. Table no. 13 shows the residues that retained their H-bonds.

S.No	**Residues involved in H bonds**	
	NKp44 residues	Hemagglutinin residues
1.	Lys33	Ile 217
2.	Ser 52	Asn216
3.	Lys33	Asn216
4.	Glu83	Arg269
5.	Glu84	Arg109
6.	Arg82	Ser110
7.	Ser119	Asn99
8.	Arg62	Asp104
9.	Ser61	Asp104
10.	Arg47	Asp101
11.	Asp97	Ser219
12.	Asp98	Ser219

Table no. 13: Residues of NKp44 and hemagglutinin involved in H bond formation after 3000ps simulation.

5. Conclusion

NK cell activation plays a very important role in triggering the immunological response. Interaction between various activating receptors and their ligands expressed by tumors cells has been known to contribute to cancer progression. However the structural information of activating receptors and their cognate ligands is very limited. Earlier attempts for searching for the ligands of NK activating receptors have not been exhaustive because in *in-vivo* and cell culture systems, it is difficult to elucidate binding efficiency of individual receptor and ligand pair and its contribution to NK cytotoxic signal since multiple receptors stochastically expressed on each NK cell additively regulate NK activity. The present study has established a computational methodology to elucidate binding efficiency of specific ligands with their cognate activating receptor. The study conducted, found a new activating ligand for NKp30 by studying its structural basis with already known ligand B7H6. The new ligand was found to be similar to tapasin which is downregulated in some tumor cells. Since the protein strongly binds to NKp30, it substantiates the hypothesis of Ag002094_TABP being a new activating ligand. The study also dealt with the elucidation of structural basis of NKp46 and NKp44 interaction with its known ligand, hemagglutinin. Residues important for the interaction of NKp44 and NKp46 were found using *in-silico* docking studies. Further experimental validation of the computational results will support the methodology and help in fishing out new activating ligands from tumor antigen pool and devising new strategies for NK cell based cancer therapy.

Chapter-2

Objective- To deduce the structural basis of HLA-G interaction with KIR2DL4 and compare its binding affinity with HLA-E, HLA-Cw3 and HLA-Cw4.

1. Introduction

HLA-G is a non classical HLA class–I antigen which is known to modulate most of the immune component cells such as NK cells, T-cells and Dendritic cells. It is restrictively expressed on fetal maternal extravillious cytotrophoblast and is capable of modulating the function of uterine natural killer cell (uNK) through NK cell receptors. The HLA-G molecule has its role in maternal–fetus immunotolerance by evading the maternal immune response as well as the pathogen infection which are threats to successful pregnancy (Le Bouteiller *et al.*,2001, Proll *et al.*,2000). Rouas-Friess *et.al* showed that trophoblast cells expressing HLA-G are protected against maternal NK cell mediated cytolysis (Rouas-Freiss *et al.*,1997). As compared to other class-I MHC molecules, HLA-G is less polymorphic and because of its structure, a very limited number of peptide are recognized and presented by it (Clements *et al.*,2005). All these aspects make HLA-G exclusively dedicated towards immune inhibition and tolerance.

KIR2DL4 (CD 158D), a member of killer cell immunoglobulin-like receptor family is constitutively expressed by all NK cells and on all KIR haplotypes (Rajagopalan *et al.*,1999). The only known ligand for KIR2DL4 is a non classical MHC class–I molecule, HLA-G. Accumulation of soluble form of HLA-G in $KIR2DL4^{+}$ endosomes suggested soluble HLA-G as its natural ligand. However no direct binding was detected by surface plasmon resonance (Boyson *et al.*,2002) which might be due to the low intrinsic activity, as has been the case of activating form of KIR and their potential MHC-I ligand (Long *et al.*,2000). The physiological relevance of HLA-G has been shown by the presence of soluble HLA-G in the human embryo culture supernatants after *in-vitro* fertilization (IVF) which lead to successful pregnancy while disorders of pregnancy like pre-eclampsia and recurrent spontaneous abortion have been observed in case of reduced levels of HLA-G in maternal circulation (Rizzo,R. *et al.*,2010). Rajagopalan *et al.* in 2006 showed that soluble forms of HLA-G shed from the cell surface of the tranfected cells and get accumulated in $KIR2DL4^{+}$ endosomes. The interaction of KIR2DL4-HLA-G has led the elaboration of its role played by eliciting proinflammatory/proangiogenic responses leading to vascular remodeling during pregnancy (Rajagopalan *et al.*,2006; 2012). However the ambiguities regarding the interaction pattern of the two proteins still remains unsolved as no co crystallized structure has been deduced yet. Study conducted here attempts to elucidate the structural basis of binding of KIR2DL4 with its known ligand HLA-G and compare the binding affinity of KIR2DL4 with other HLA molecules involving HLA E, HLA Cw3 and HLA Cw4. We have employed a computational approach to find the residues playing a key role in KIR2DL4-HLA-G interaction and interaction pattern with other HLA molecules. The structure of KIR2DL4 was modeled with the help of modeling software. The modeled structure was then used to carry out protein–protein docking with HLA-G, HLA E, HLA Cw3 and HLA Cw4 to observe the interaction pattern of the proteins. Since docking gives interactions in static state, molecular dynamic simulations were carried out in order to obtain a dynamic perspective. The interaction pattern observed provided a detailed view of one of the most elusive pair of interacting proteins. Also, in the absence of crystallized structure, the study conducted here will provide

mechanistic insights of KIR2DL4-HLA-G interaction which plays a pivotal role in immune-tolerance during pregnancy.

2. Review of Literature

2.1 KIR2DL4

The killer cell immunoglobulin-like receptor (KIR) family of activating and inhibitory receptors expressed by natural killer (NK) cells regulates their responsiveness to signals received from their environment. NK cells respond to contact with other cells including tumor cells or virus-infected cells, and to soluble mediators such as cytokines, chemokines or other soluble ligands. KIR regulates the activation state of NK cells upon recognition of their major histocompatibility complex (MHC) ligands on the surface of target cells (Long. E, 2008). There is genetic evidence that combinations of KIR and MHC genes contribute directly to different aspects of immunity, such as resistance to infections, susceptibility to autoimmune diseases, transplantation outcomes, and disorders of pregnancy (Parham, 2005).
KIR2DL4 (CD158d), the anchor gene in the middle of the KIR complex, is characterized by its low polymorphism, high degree of conservation among primates, and by its central location among the highly variable KIR family members. There are KIR2DL4 alleles with either 9 or 10 consecutive adenines in exon 6, which encodes the transmembrane domain. This 9A/10A transmembrane genetic polymorphism can result in a truncated receptor encoded by 9A, the function of which is unclear (Goodridge *et al.*,2003). Unlike other KIR genes that display variegated expression among individual NK cells, KIR2DL4 is constitutively expressed by all NK cells and on all KIR haplotypes (Rajagopalan and Long, 1999).

Among KIR family members, KIR2DL4, which was assigned the new CD designation CD158d (Andre´, P. *et al.*,2001), displays unusual characteristics. First, KIR2DL4 carries a single ITIM (the tyrosine of the second ITIM is substituted by a cysteine residue). Second, in addition to the presence of an inhibitory motif, KIR2DL4 contains a charged residue in its transmembrane region, suggesting the possibility of an activating function for this receptor (Selvakumar, A. *et al.*,1996). These two properties may explain earlier observations on the function of KIR2DL4. Indeed, both inhibitory (Ponte, M *et al.*,1999) and activating (Rajagopalan, S. *et al.* 2001) functions have been described for KIR2DL4. Third, the mRNA of KIR2DL4 is present in every NK cell, in contrast to all other KIR that are expressed in overlapping subsets of NK cells (Valiante, N *et al.*,1997, Cantoni, C. *et al.*,1998). Fourth, the two Ig-like extracellular domains of KIR2DL4 and of KIR2DL5 have the unusual D0-D2 configuration, in contrast to the usual D1-D2 and D0-D1-D2 organization of Ig domains in other KIR2D and KIR3D receptors, respectively. Finally, KIR2DL4 binds to cells expressing HLA-G (Rajagopalan, S. *et al.* 1999), a nonclassical HLA class I molecule expressed by trophoblast cells that invade the maternal decidua (Kovats, S. *et al.*,1990), by activated monocytes (Yang, Y. *et al.*, 1996;Moreau, P.,1999), by thymic epithelial cells (Crisa *et al.* ,1997) and by certain tumor cells (Carosella *et. al.*,2000).

The only known ligand for KIR2DL4 is the non-classical MHC class I molecule HLA-G. The soluble form of HLA-G may be its natural ligand as it accumulates in KIR2DL4+ endosomes and induces endosomal signaling. Soluble HLA-G can be generated either by shedding as a result of the metalloprotease-mediated cleavage of the extracellular domain of the transmembrane isoform HLA-G1 (Park *et al.*, 2004), or by alternative RNA splicing to produce the soluble form known as HLA-G5. Transfected cells expressing a high level of cell surface HLA-G1 were shown to bind recombinant Ig-fusion proteins of KIR2DL4 (Ponte *et al.*, 1999; Rajagopalan and Long, 1999). This binding was blocked by monoclonal antibodies (mAb) to HLA-G and to KIR2DL4 (Rajagopalan *et al.*, 2006).

However, so far, no direct binding of soluble forms of HLA-G to KIR2DL4 has been detected as measured by surface Plasmon resonance (Boyson *et al.*, 2002). This could be due to an intrinsic low affinity, as has been the case with activating forms of KIR and their potential MHC-I ligands (Long and Rajagopalan, 2000). Tetrameric HLA-G binds to its ligand ILT4 (CD58d/LILRB2) on monocytic cells, but not to ILT2 (CD85j/LILRB1) or KIR2DL4 on NK cells (Allan *et al.*, 1999). This is likely due to the very low surface expression of ILT2 and KIR2DL4 in primary NK cells. HLA-G can be expressed as monomers or disulphide linked homodimers on the NK cell surface (Apps *et al.*, 2007). While ILT2 binds preferentially to dimeric HLA-G (Shiroishi *et al.*, 2006), it is not known if KIR2DL4 favors HLA-G monomers over dimers. The crystal structure of dimeric HLA-G and modeling of KIR2DL4–HLA-G interactions indicate that steric constraints would prevent KIR2DL4 from interacting with HLA-G in its dimeric form (Clements *et al.*, 2007). It has been reported that NK cells produced cytokines in the presence of transfectants of 221 cells expressing the HLA-G homodimer, but not with those expressing the HLA-G C42S mutant monomer (Li *et al.*, 2009). Since both monomers and dimers are present on the cell surface of 221 cells expressing wild-type HLA-G, the issue is not resolved. Moreover, Fab fragments of an agonist antibody to KIR2DL4 can activate NK cells indicating that a monomeric ligand can work (Rajagopalan *et al.*, 2006).

Both soluble HLA-G5 and HLA-G shed from the cell surface of transfected cells were accumulated into endosomes that contain KIR2DL4 (Rajagopalan *et al.*, 2006). This was detected by confocal microscopy as co-localization of soluble HLA-G and KIR2DL4 in the same vesicular compartments. There was no accumulation of soluble HLA-C under the same conditions. Evidence for direct binding was obtained by showing that endocytosis of soluble HLA-G was blocked in the presence of a soluble KIR2DL4-Ig fusion protein, while a soluble KIR2DL1-Ig fusion protein did not block uptake of soluble HLA-G (Rajagopalan, 2010). It is likely that transient passage of KIR2DL4 at the cell surface, either by newly synthesized KIR2DL4 or by recycling of endosomal KIR2DL4, is sufficient to capture soluble HLA-G and transport it to endosomes.

2.2 Relevance of KIR2DL4 and HLA-G interaction

HLA-G is unusual among HLA molecules in its unique pattern of expression in healthy individuals. Unlike classical MHC-I molecules that are widely expressed on most somatic cells, HLA-G expression is restricted to fetal trophoblast cells at the maternal– fetal interface. However, there is evidence of up-regulation of HLA-G mRNA in response to transformation, neovascularization, inflammation, and infection (Carosella *et al.*, 2008). There is also evidence for increased soluble HLA-G secretion in the serum of patients with malignancies such as melanoma, glioma, ovarian, and breast cancer (Rebmann *et al.*, 2003). Increased levels of circulating sHLA-G have also been detected in viral infections such as HIV-1 (Huang *et al.*, 2010). In the transplantation setting, induction of HLA-G expression correlates with increased transplant acceptance. In healthy individuals, the best-documented evidence of HLA-G protein expression occurs on fetal trophoblast cells that invade the maternal decidua during early pregnancy (Moffett and Loke, 2006). Known receptors for HLA-G are found on NK cells (KIR2DL4 and ILT2) and on monocytic cells (ILT2 and ILT4). All these receptors are present on innate immune cells that comprise the majority of lymphocytes at the maternal–fetal interface in early pregnancy (Moffett-King, 2002). The presence of soluble HLA-G in human embryo culture supernatants after in vitro fertilization (IVF) correlates with successful pregnancy and reduced levels of HLA-G in maternal circulation has been reported in disorders of pregnancy, such as pre-eclampsia and recurrent spontaneous abortion (Rizzo *et al.*, 2010). The earlier view that HLA-G is tolerogenic by protecting the fetus from attack by maternal NK cells is losing support, as newer findings do not support the role of HLAG as a tolerance molecule in this context (Li *et al.*, 2009). In addition to HLA-G, HLA-C, and HLA-E are present on fetal trophoblast cells. Both HLA-C and HLA-E can block NK lysis upon recognition of combinations of inhibitory KIR and CD94/NKG2A receptors expressed by all uterine NK cells (Moffett-King, 2002). Moreover, much of the inhibitory function ascribed to HLA-G is now recognized to be due to HLA-E, since HLA-G expression in cells promotes HLA-E co-expression. This occurs upon binding of the HLA-G signal peptides to the HLA-E peptide-binding groove, resulting in the proper assembly and cell surface expression of HLA-E. In this way, expression of HLA-E on trophoblast cells allows global inhibition of NK cytotoxicity through CD94/NKG2A. Early reports on the effects of HLA-G on NK cells used total peripheral blood mononuclear cells (PBMC) and not purified NK cells to assess NK cell lytic activity (RouasFreiss *et al.*, 1997; Riteau *et al.*, 2001). The inhibitory effect of HLA-G was later shown to be on T cells and not on NK cells. Thus, while HLA-G inhibits the proliferation and cytotoxic activity of T cells, it activates decidual NK cells to secrete cytokines and to proliferate (van der Meer *et al.*, 2004; 2007).

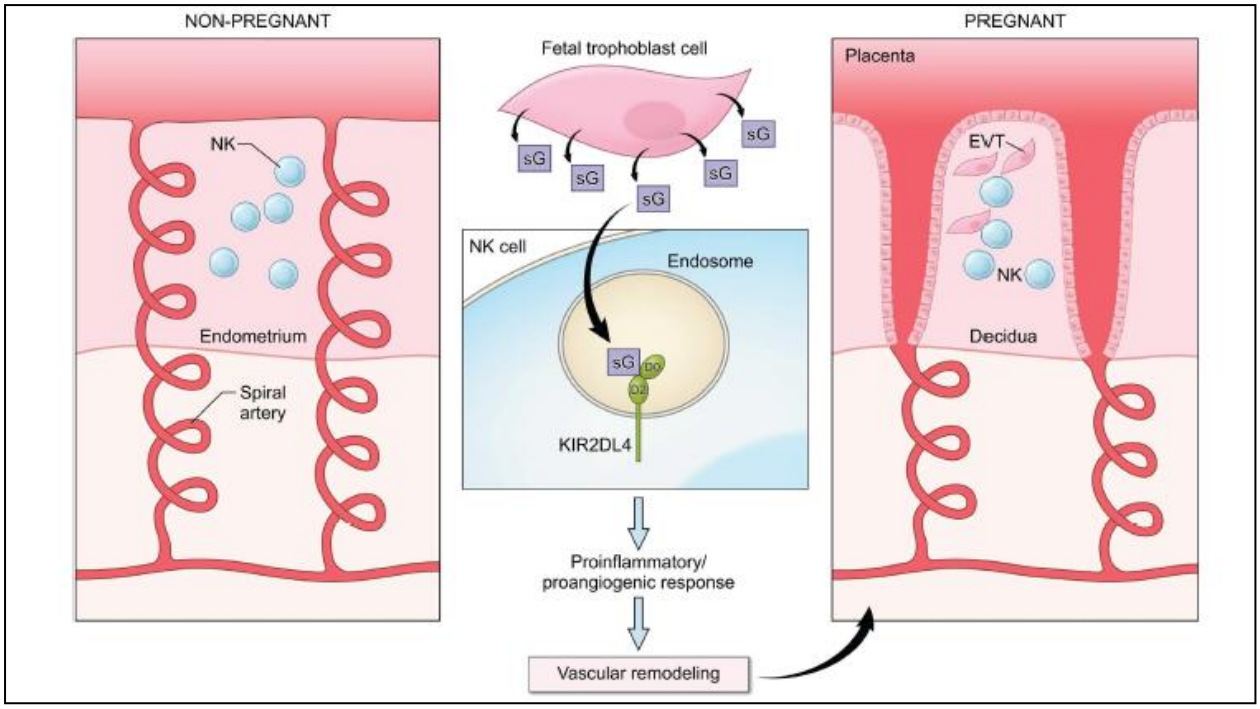

Figure a: Potential role of KIR2DL4–HLA-G interactions in early pregnancy. NK cells are abundant in the non-pregnant endometrium (leftpanel) in the secretory phase of the menstrual cycle. In early pregnancy (right panel), interactions between fetal extra villous trophoblast cells (EVT) and NK cells in the deciduas contribute to the remodeling of the spiral arteries to allow increased blood supply to the fetus. Fetal trophoblast cells secrete soluble HLA-G(sG),which can be endocytosed by KIR2DL4 into endosomes. Endosomal signaling then results in a sustained proinflammatory/proangiogenic secretory response that may promote the vascular changes seen in early pregnancy. (Courtesy Rajagopalan *et al.*,2012)

3. Material and Method

3.1 KIR2DL4 modeling

A 263 long amino acid sequence of KIR2DL4 of human origin was retrieved from NCBI (accession no. = AAW32132.1). Since the crystal structure of KIR2DL4 was not available, the protein was modeled using a hybrid modeling server named Phyre2 (Soding, J. 2005). The platform incorporates *ab-initio* folding simulation called Poing[2] to model regions of proteins with no detectable homology to the known structures (Jefferys *et al.*,2010). The modeled structures was then subjected to energy minimization by using pdb swissviewer which involve a version of GROMOS 42B1 force field (Guex *et al.*,1997; Gunsteren *et al.*,1996).The force field allows the evaluation of energy of a structure as well as repair distorted geometries through energy minimization. Following minimization the quality of the modeled structure was analyzed on the basis of various structural properties using ERRAT (Luthy *et al.* 1992) and Ramachandran plot **(**Morris *et al.*,1992**)**. The model was further refined and stabilized using molecular dynamics (MD) simulations. Desmond Molecular Dynamic System (Guo *et al.*,2010; Shaw, D.E 2010) with Optimized Potential for Liquid Simulations (Jorgensen *et al.*,1996; Kaminski *et al.*,2001) all atom force field was used to study the dynamic stability of the modeled protein. The missing residues were manually fixed. H-bonds were optimized by using H-bond assignment. The prepared complex was solvated in a triclinic periodic box of SPC water and then neutralized with appropriate number of counter-ions. The distance between the wall of the box and the complex was kept as 10 Å to prevent the interaction with its own periodic image. The prepared system was then subjected to energy minimization to a maximum of 3000 steps using a steepest decent method until a gradient threshold (25 kcal/mol/Å) was reached. The equilibrated system was used to carry out further MD Simulations for 3000 ps at a constant temperature of 300K and constant pressure of 1atm with a time step of 2 fs. Smooth particle Mesh Edwald method was used to calculate long distance electrostatic interactions. A 9 Å cutoff radius was used for coloumbic short range interaction cutoff-method. Frames of the trajectory were captured every 4.8 ps of the time interval.

3.2 Ligand preparation

The crystallized structures of HLA-G, HLA-E, HLA Cw3 and HLA Cw4 are available in RCSB Protein Data Bank (Berman *et al.* 2000) with PDB IDs- 1YDP, 3CII, 1EFX and 1IM9 respectively (Clements *et al.*2005, Kaiser *et al.* 2008 Boyington *et al.*, 2000 ;Fan *et al.*, 2001). The structures were present in complexed form with their respective receptors. These structures were prepared using Viewerlite, a molecular viewer suite by Accelerys, by deleting water molecules and other proteins complexed with them. These structures were then subjected to minimization using energy minimization protocol of pdb Swissviewer. Energy minimization prepares a protein by minimizing the net forces on atoms, hence bringing it to a stable molecular state.

3.3 Molecular Docking-HADDOCK Server

Protein–protein docking was performed using the Easy Interface docking protocol of Haddock Server (Sjoerd J. *et al.*,2007) which requires parameters like active residues and passive residues of the interacting proteins. Haddock (High Ambiguity Driven Protein-Protein Docking) is information driven flexible docking approach for modeling of biomolecular complexes. The approach adopted by the program is different from *ab-initio* docking protocols as it takes information from identified or predicted protein interfaces in ambiguous interaction restraints (AIRs) to drive the docking process (Dominguez *et al.* 2003). The program makes use of the already existing experimental and bioinformatics data to accomplish docking process (van Dijk *et al.*,2005). In this study, Easy Interface module of HADDOCK was used, which requires proteins to be submitted in .pdb format along with mentioning of active (directly involved in interactions) and passive residues (surrounding surface residues).

3.4 Analyzing site of Docking

3.4.1 KIR2DL4

The docking site for KIR2DL4 was determined by sequence alignment with other KIR molecules. The sequence of KIR2DL4 was submitted for Position specific iterated BLAST and its identical regions with other KIR molecules (KIR2DL1, KIR2DL3 ,KIR2DL2) were determined. These regions were then structurally compared with the binding regions of other KIR molecules with their respective ligands. The overlapping regions of KIR2DL4 and other KIR molecules (which are involved in binding regions) were taken as the active site residues of KIR2DL4 while amino acids surrounding the active region were selected as passive residues.

3.4.2 HLA Molecules

The site of docking for HLA-G molecule was determined by previous cited literature. Yan WH *et al.* suggested that residues Met76 and Gln79 in HLA-G alpha domain play a very critical role in recognition of KIR2DL4. Their results showed that mutating these residues to Ala affected the binding affinity of KIR2DL4-HLA-G (Yan *et al.*, 2005.). Hence the docking was performed by selecting these residues as active.

The docking site for HLA E, HLA Cw3 and HLA Cw4 was selected by studying their respective complexes in PDB (Protein Data Bank). HLA E is present in complex with NKG2A [PDB ID =1EFX] and the residues important for its interaction with the receptor

were taken as residues of active site while performing docking with KIR2DL4. Similarly, the active site residues of HLA Cw3 and HLA Cw4 were examined by studying their complex with KIR2DL2 [PDB ID = 3CII] and KIR2DL1 [PDB ID = 1IM9] respectively. Residues which were located in a continuous stretch near the predicted interaction interface for which no information was available were defined as passive.

4. Results and Discussion

4.1 3D Structure of KIR2DL4

The modeled structure obtained from Phyre2 was subjected to Molecular dynamic simulations. Desmond Molecular Dynamic System was used for 15 ns simulation run to obtain a stable state of the modeled structure as shown in figure 1. The figure shows that the structure deviated from its initial state but attained stability at the latter part of the run. The structure was almost stable from 7 to 15 ns. Figure 2 and 3 show Ramachandran and ERRAT plot respectively. These plots were used to test the quality of the structure obtained after the simulation run. Ramachandran plot showed that 72.8 % of the residues were in the favorable region and only 1.9 % of the residues were in the disallowed region. None of the residues in the disallowed region were overlapping with the residues of the site of interaction or involved in interaction with any functionally important residue of KIR2DL4. The ERRAT plot also showed that the overall quality of the modeled structure improved from 49.412 to 69.332 %. An RMSD of 2.259 Å was observed when pre MD and post MD structure of KIR2DL4 were aligned (shown in figure 4).

The RMSD curve showed that the trajectory attained a stable state after 7 ns. However a very slight deviation in the structure was seen after 15 ns. For the docking and interaction analysis an average structure from the time frame of 7000 to 15000 ps was taken.

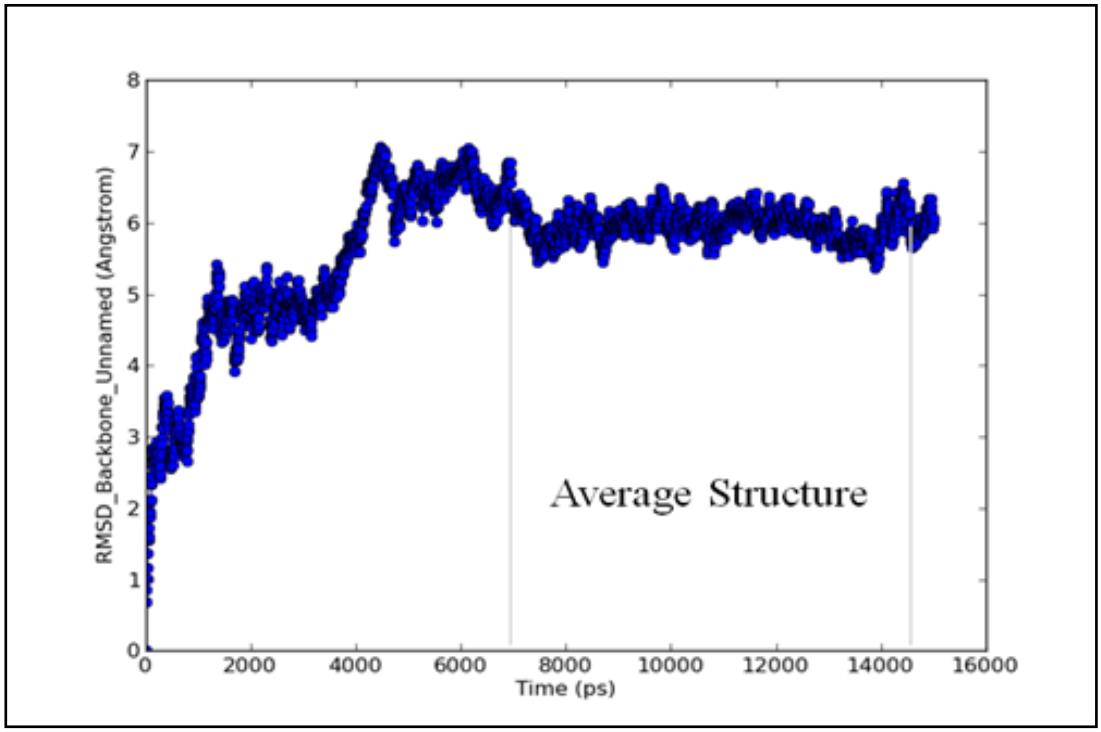

Figure 1: RMSD plot of KIR2DL4 modeled structure for 15 ns simulation run.

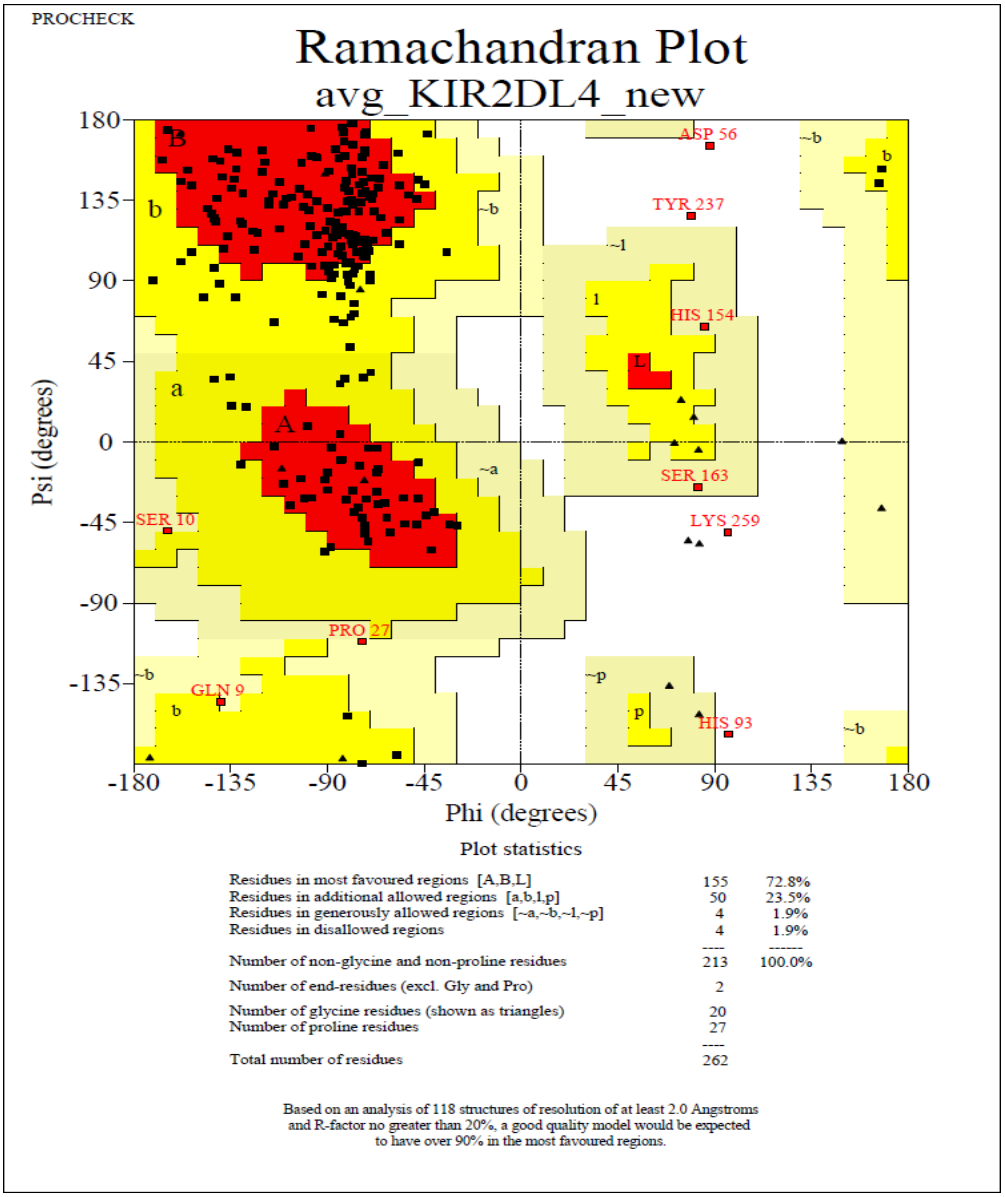

Figure 2: Ramachandran plot of the KIR2DL4 after 15ns of simulation.

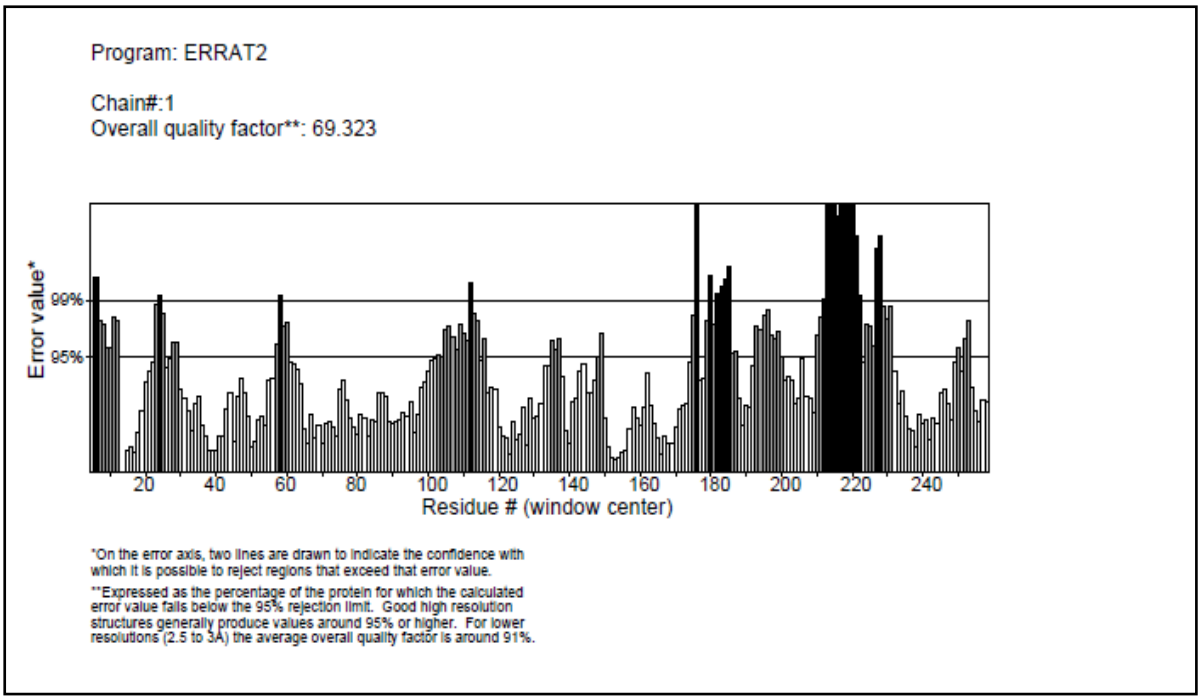

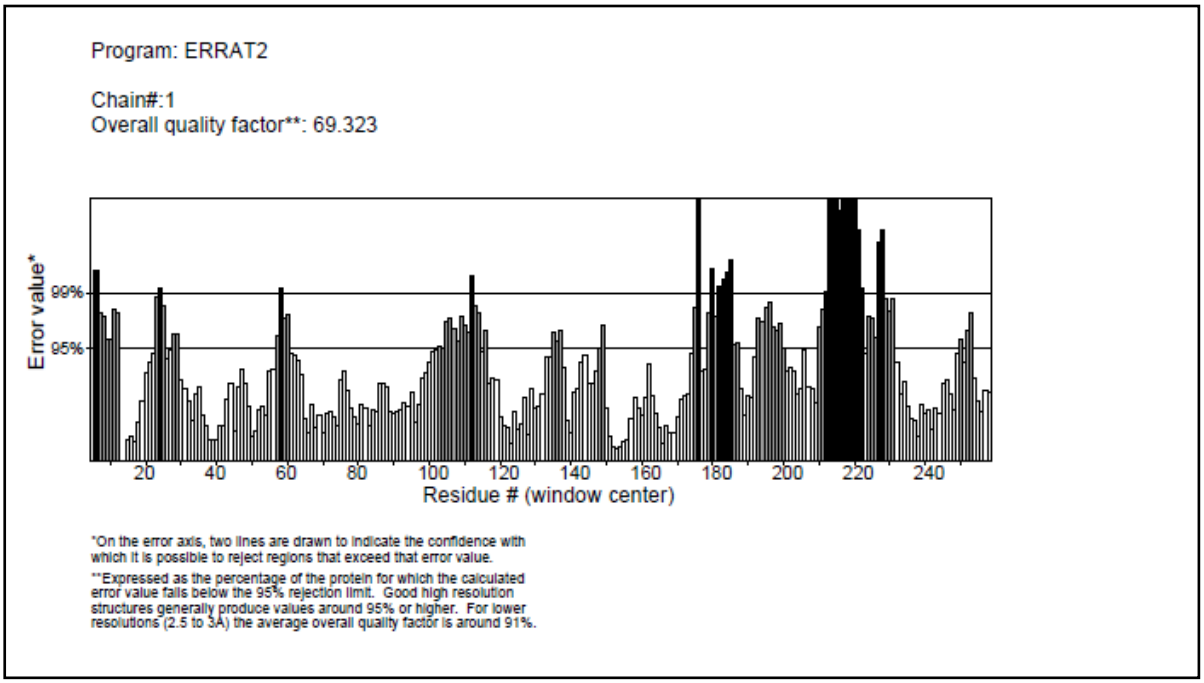

Figure 3: Errat plot of the pre and post Molecular Dynamics KIR2DL4 structure which shows that an overall quality factor has improved from 49.412 to 69.323.

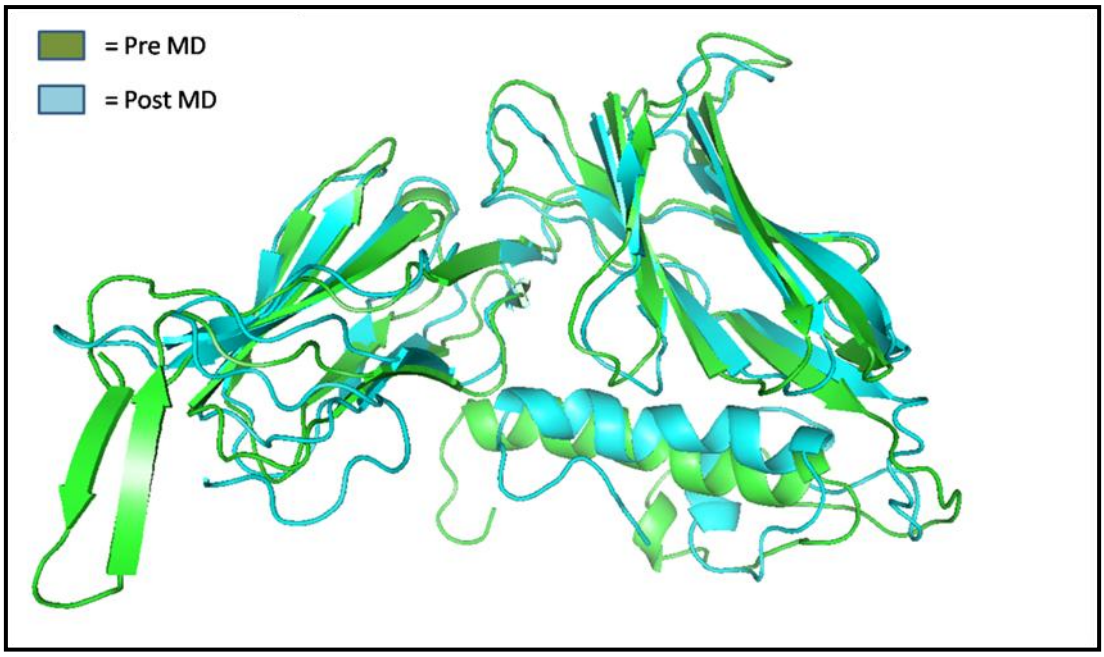

Figure 4: Alignment of Pre MD and Post MD structure of KIR2DL4. An RMSD of 2.259 Å was observed.

4.2 Molecular Docking

Easy Interface docking protocol of HADDOCK was used for carrying out all the dockings. The information provided by the AIRs (Dominguez *et al.*,2003), is used for driving the docking process. The approach not only reduces the necessary search but also increases the chances of unique solutions. The AIRs are defined in terms of active and passive residues. While the active residues are those residues which are important for the interactions, passive residues are defined as the solvent-accessible neighbors of active residues.

4.2.1 KIR2DL4- HLA-G

The active residues of HLA-G were defined with the help of already proven experimental results of Yan WH. *et.al.* They suggested that KIR2DL4 interacts with HLA-G with key residues Met76, Gln79 and Thr80, absence of which significantly reduces the binding affinity (Yan *et al.*,2005). The solvent accessible neighbors of these residues were selected as passive residues. For defining active residues for KIR2DL4, PSI BLAST was performed and compared with all other KIRs present in RCSB PDB .The conserved regions obtained were

then compared with binding site of other KIR molecules. The residues present in the overlapping regions were defined as the active sites while passive were taken as their surrounding counterparts.

The results obtained from HADDOCK Easy Interface, were in the form of 7 clusters having 172 structures. These were obtained from a three step protocol involving an initial stage of rigid docking to generate 1000 structures, followed by semi-flexible simulated annealing in torsion angle space of 200 best structures in terms of intermolecular energy (sum of van der Waals, electrostatic, and ambiguous interaction restraints energy terms). Final stage of the docking protocol involves inclusion of water in calculations to improve the energy of the structures. Clustering was done using a 3.5 Å RMSD cut-off and ranked according to their average interaction energies (sum of Electrostatic, Van der Waal and Desolvation energy) and their average buried surface area according to the HADDOCK protocol. Out of these 7 clusters, the one with the lowest HADDOCK score was chosen and from that cluster the best structure was selected for interaction analysis. Table no. 1 show that the HADDOCK score for the best cluster was -88.3+/-6.5. The cluster had 65 structures and the RMSD value from the lowest energy structure came out to be 1.2+/-0.7 Å. The statistical parameter, Z score was also calculated for the cluster which indicates how many standard deviations from the average this cluster is located in terms of score, which was observed to be high (Z= -1.7).

The HADDOCK server also returns a graphical representation of clustering done on various parameters including graphs of HADDOCK score v/s interface ligand RMSD, ligand RMSD, Van Der Waal v/s liagnd RMSD. One of the graphs significant for analysis of the clustering is HADDOCK v/s i-l-RMSD graph as it supplies information of the structure of lowest HADDOCK score. Figure 5 shows HADDOCK score in atomic units (a.u.) and RMSD in Å, the cluster with lowest energy, shown in red.

HADDOCK score	-88.3 +/- 6.5
Cluster size	65
RMSD from the overall lowest-energy structure	1.2 +/- 0.7
Van der Waals energy	-39.1 +/- 6.0
Electrostatic energy	-297.4 +/- 27.6
Desolvation energy	10.2 +/- 9.1
Restraints violation energy	0.8 +/- 0.63
Buried Surface Area	1360.8 +/- 81.3
Z-Score	-1.7

Table no. 1:Results obtained from HADDOCK for KIR2DL4-HLA-G

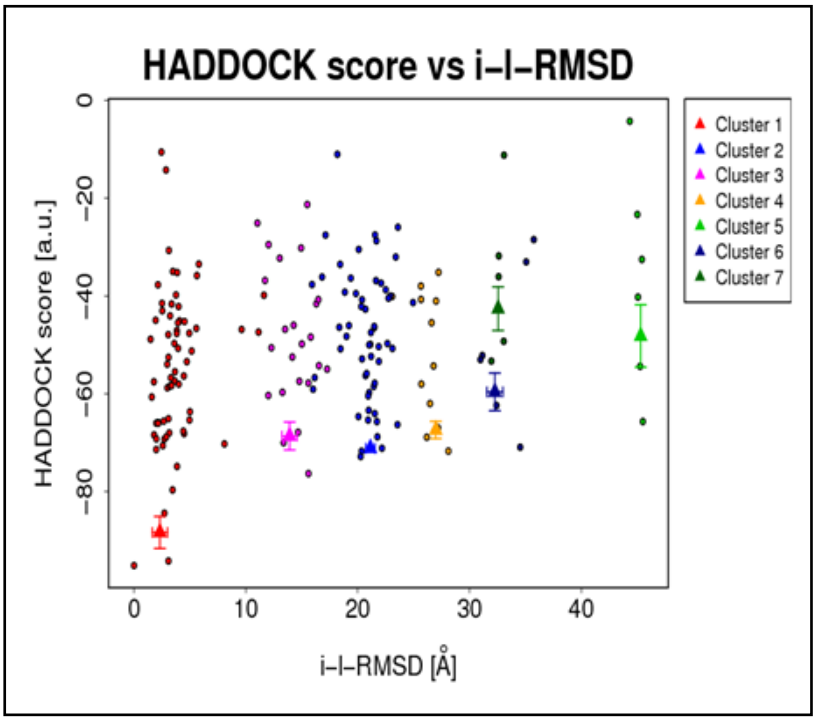

Figure 5: The graph showing the clustering of structures of KIR2DL4-HLA-G on the basis of HADDOCK Score

Interactions and Residues important in KIR2DL4-HLA-G association

The best structure from the cluster with lowest HADDOCK score was selected for interaction analysis. The interaction analysis and molecule visualization was done with the help of Viewer Lite, molecular viewer by Accelerys and Pymol. It was observed that the active residues as mentioned by Yan W.H. *et al.*, were important for the binding of HLA- G with its receptor KIR2DL4. Figure 6 shows the complex of KIR2DL4 and HLA-G with their residues highlighted in green. This H-Bonds visualization and the measurement of distance between the H bond forming atoms was done using Pymol. Table no. 2 lists the 10 H-bonds between the residues in the complex of KIR2DL4-HLA-G. Apart from the residues cited in the literature many other residues were forming strong H- bonds, suggesting their possible role in stabilizing the binding of these two proteins. Figure 6 shows all the residues of KIR2DL4 and HLA-G involved in H bonds. It was observed that Gln79 (cited as a key residue of HLA-G for KIR2DL4 interaction) formed 2 H bonds with Tyr113 and Glu195.

S.No.	Residues of KIR2DL4	Residues of HLA-G	H bond disatance (Å)
1.	Asp 56	Asn 86	2.0
2.	Gly 57	Asn 86	2.3
3.	Ala 80	Glu 89	1.8
4.	Thr 79	Glu 89	1.9
5.	Tyr 113	**Gln 79**	1.8
6.	Ser 141	Lys 146	1.8
7.	Asp 143	Lys 146	1.6
8.	Asp 143	Tyr 84	1.7
9.	His 190	Arg 145	2.6
10.	Glu 195	**Gln 79**	1.8

Table no. 2: Residues of KIR2DL4 which forms H bonds with HLA-G along with their H Bond distance

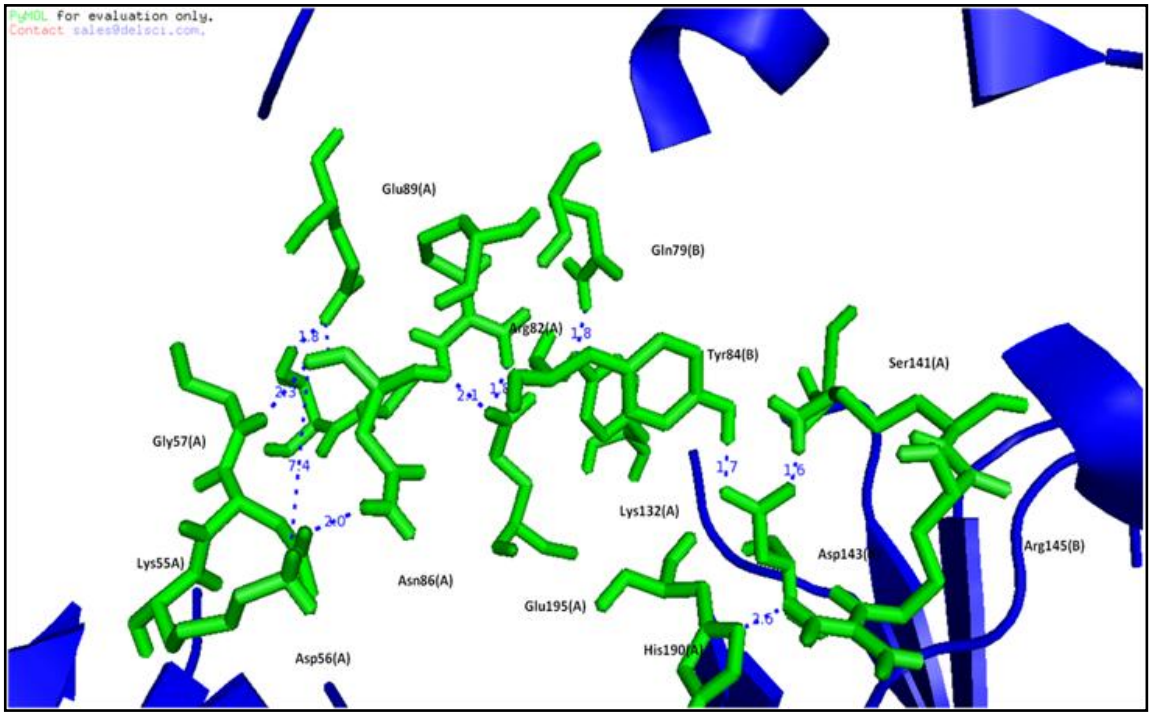

Figure 6: H bond forming residues of HLA-G and KIR2DL4

4.2.2 KIR2DL4-HLA-E

The study also deals with comparison of binding affinity of different class I HLA molecules with KIR2DL4. HLA-E is an important player in pregnancy and apart from expression on fetomaternal surface, it is widely distributed among T-cells, B-cells, activated T lymphocytes and various other cells (Houlihan *et al.*,1995). To determine its binding efficiency with KIR2DL4, the pair of proteins was subjected to Easy Interface HADDOCK docking protocol.

The docking results show a very low HADDOCK score for HLA-E and KIR2DL4 interaction. 11 clusters were obtained having 147 structures and representing 73.5 % of the water-refined models generated by HADDOCK. Out of these 11 clusters the top clusters was chosen with the lowest HADDOCK score of -69.7+/-4.9. The cluster had 36 structures and the RMSD value from the lowest energy structure came out to be7.9 +/- 0.3 Å .The statistical parameter Z score was also calculated for the cluster which indicates how many standard deviations from the average this cluster is located in terms of score, which was observed to be high (Z= -1.6). Table no. 3 shows all other energy scores obtained from KIR2DL4 and HLA-E docking.

The HADDOCK server also returns a graphical representation of clustering done on various parameters including graphs of HADDOCK score v/s interface ligand RMSD, ligand RMSD, Van Der Waal v/s liagnd RMSD. One of the graphs significant for the analysis of clustering is HADDOCK v/s i-l-RMSD graph as it supplies the information of the structure of lowest HADDOCK score. Figure 7 shows HADDOCK score in atomic units (a.u.) and RMSD in Å, the cluster with lowest energy, shown in red.

HADDOCK score	-69.7 +/- 4.9
Cluster size	36
RMSD from the overall lowest-energy structure	7.9 +/- 0.3
Van der Waals energy	-23.2 +/- 4.3
Electrostatic energy	-368.9 +/- 31.0
Desolvation energy	24.1 +/- 7.8
Restraints violation energy	32.9 +/- 1.70
Buried Surface Area	1314.8 +/- 119.0
Z-Score	-1.6

Table no. 3: Results obtained from HADDOCK for KIR2DL4-HLA-E interaction

Table no. 4 shows the residues of KIR2DL4 and HLA-E which were bound by H-bonds. The distances of these H-bonds were also calculated by Pymol. It was seen that the residues of KIR2DL4 which were involved in H-bond interactions were different as compared to the complex of KIR2DL4-HLA-G. The interactions of residues play a key role in HADDOCK score. Weak affinity of proteins towards each other is reflected by the low HADDOCK score and less number of bonding residues. Figure 7 shows the interacting residues of HLA-E with KIR2DL4.

S.No.	Residues of KIR2DL4	Residues of HLA-E	H-bond disatance (Å)
1.	Asp 56	Asn 79	2.2
2.	Asp 56	Glu89	2.3
3.	Ala 80	Glu 89	1.8
4.	Pro 79	Arg 79	2.4
5.	Tyr 113	Arg75	1.8
6.	Asp 142	Lys 146	1..7
7.	Ser 163	Ala 150	1.6
8.	Asp 56	Arg 79	2.7
10.	Glu 195	Arg 75	2.2

Table no. 4: Residues of KIR2DL4 which form H bonds with HLA-E along with their H-bond distances

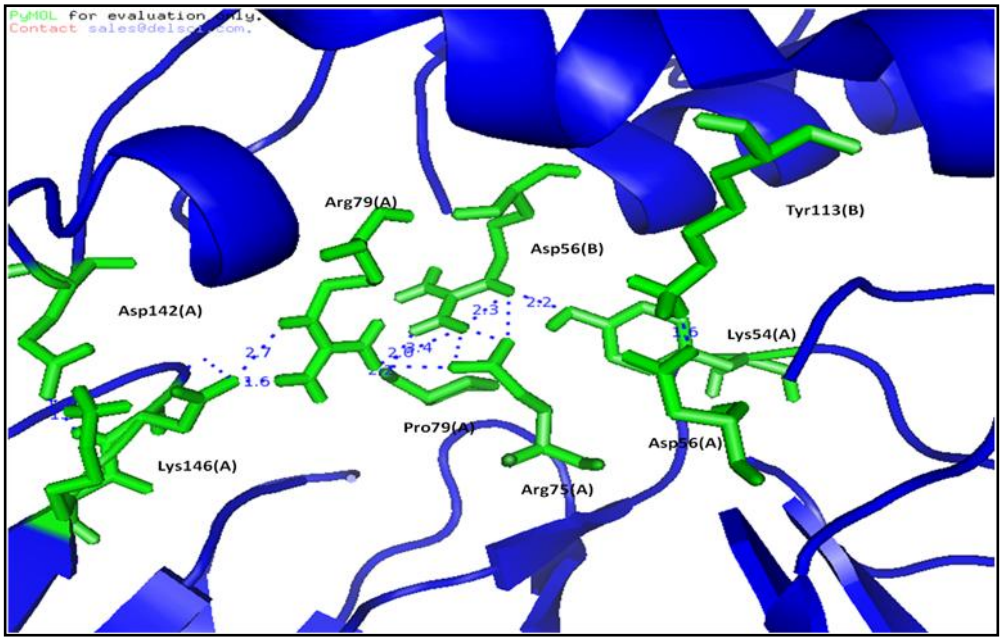

Figure 7: H-bond forming residues of HLA-E and KIR2DL4

HLA-E specifically interacts with CD94/NKG2A which results in the inhibition of NK cells (Carretero *et al.* 1998).The previous experimental validations have proved its weak affinity towards KIR2DL4. As suggested by Rajagopalan *et al.* in 1999, KIR2DL4 specifically interacts with HLA-G and not HLA-E, the experimental study carried out here validated the procedure by showing weak binding affinity of HLA-E and KIR2DL4. A low HADDOCK score proved that KIR2DL4 has a weak binding affinity towards HLA-E. Further the H-bonds formed were lesser in number when compared to the binding pattern of KIR2DL4-HLA-G.

4.2.3 KIR2DL4-HLA-Cw3

PDB structure of HLA-Cw3 in complex with KIR2DL2 was available (Boyington JC *et al.* 2003). The interaction between fetal HLA-C molecules and KIRs expressed on uterine NK cells is thought to play a key role in the development of the placenta and the regulation of fetal growth (Trowsdale J. *et al.* 2008). There are evidences of importance of HLA C/KIR binding as uterine NK cells preferentially express HLA-C interacting KIRs (Sharkey AM *et al.* 2008). However experimental studies to identify the binding of KIR2Dl4 with HLA-C have not been carried out. The binding affinity of HLA-Cw3 with KIR2DL4 was determined by subjecting the proteins to HADDOCK docking protocol. The active site residues for HLA-Cw3 were determined from the PDB structure. The complex of HLA-Cw3-KIR2DL2 was examined to identify the key interacting residues of HLA-Cw3. These residues were then marked as active residues while submitting it for docking. All other solvent accessible neighbors of active residues were marked as passive. The active site of KIR2DL4 was kept the same as mentioned in other docking protocols.

The HADDOCK result was in the form of 4 clusters having 187 structures which represented 94.5 % of the water-refined models, the server generated. Out of these 11 clusters the top clusters with the highest HADDOCK score of -103.9 +/- 9.6 was chosen. The cluster had 155 structures and the RMSD value from the lowest energy structure came out to be 1.5 +/- 1.3 Å. The statistical parameter Z score is also calculated for the cluster which indicates how many standard deviations from the average this cluster is located in terms of score, which was observed to be high (Z= -1.5) (as shown in table no. 5).

HADDOCK score	-103.9 +/- 9.6
Cluster size	155
RMSD from the overall lowest-energy structure	1.5 +/- 1.3
Van der Waals energy	-43.0 +/- 6.5
Electrostatic energy	-332.9 +/- 88.9
Desolvation energy	5.5 +/- 9.1
Restraints violation energy	1.4 +/- 1.83
Buried Surface Area	1817.0 +/- 210.3
Z-Score	-1.5

Table no. 5: Results obtained from HADDOCK for KIR2DL4-HLA-E interaction

The HADDOCK server also returns a graphical representation of clustering done on various parameters including graphs of HADDOCK score v/s interface ligand RMSD, ligand RMSD, Van Der Waal v/s liagnd RMSD. One of the graphs significant for analysis of the clustering is HADDOCK v/s i-l-RMSD graph as it supplies the information of the structure of lowest HADDOCK score. Figure 8 shows HADDOCK score in atomic units (a.u.) and RMSD in Å, the cluster with lowest energy, shown in red.

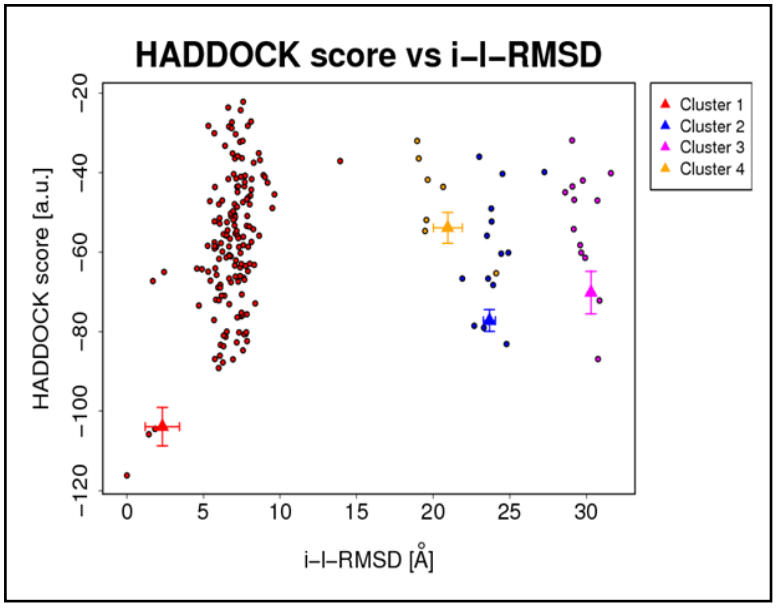

Figure 8: Clustering of structures of complex HLA-Cw3-KIR2DL4 obtained from HADDOCKTable no. 6 shows the residues which were involved in the H bond interaction. It was observed that some residues of KIR2DL4, forming H bonds in KIR2DL4-HLA-Cw3 and KIR2DL4 HLA-G

complex were the same. Figure 9 shows the H-bond forming residues (highlighted in green) and the distance of the H-bonds formed. Since HADDOCK score obtained was considerably high than the HLA-G-KIR2DL4 complex, it can be proposed that KIR2DL4 interacts strongly with HLA-Cw3. Asp143 and Tyr 113 of KIR2DL4 were the common H-bond forming residues among both the complexes. The study reveals that these two residues of KIR2DL4 are very important for its interaction. Overall 11 H-bonds were formed showing a high affinity of HLA-Cw3 for KIR2DL4.

S. No.	Residues of KIR2DL4	Residues of HLA-Cw3	H bond disatance (Å)
1.	Asp 56	Asn 79	2.2
2.	Asp 56	Glu89	2.3
3.	Ala 80	Glu 89	1.8
4.	Pro 79	Arg 79	2.4
5.	Tyr 113	Arg75	1.8
6.	Asp 143	Lys 146	1..7
7.	Ser 163	Ala 150	1.6
8.	Asp 56	Arg 79	2.7
10.	Glu 195	Arg 75	2.2

Table no. 6: Residues of KIR2DL4 which forms H bonds with HLA-Cw3 along with their H Bond distance

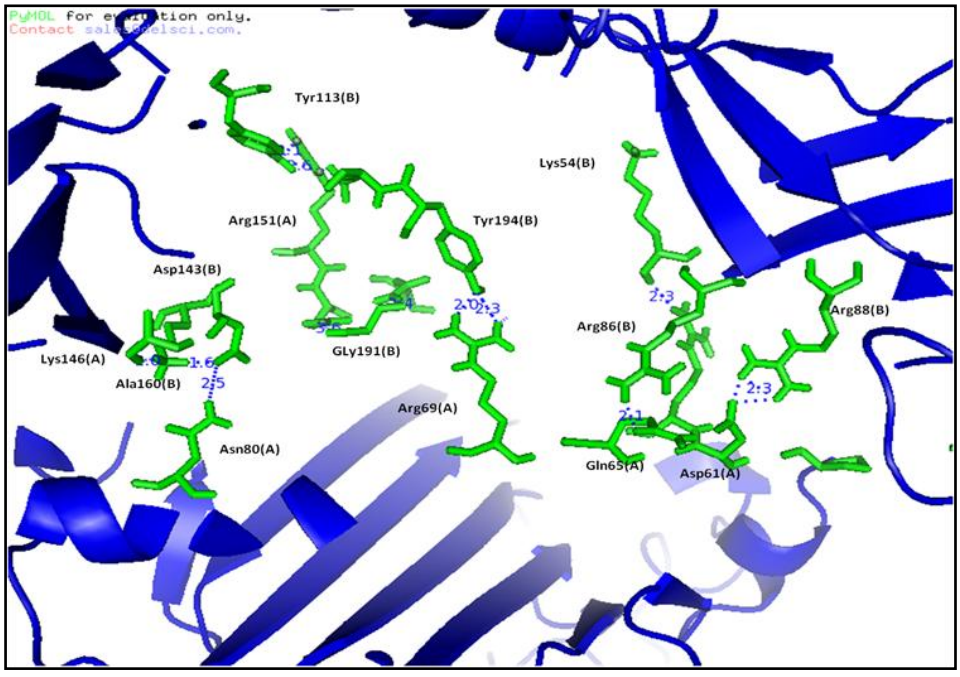

Figure 9: Residues of HLA-Cw3 and KIR2DL4 involved in H-bond interaction.

4.2.4 KIR2DL4-HLA-Cw4

KIR2DL4 gave a high HADDOCK score with HLA-Cw3, its binding affinity was also examined with HLA-Cw4. The active site for HLA-Cw4 was determined by studying its interactions with the already existing crystal structure of HLA-Cw4-KIR2DL1 (Fan *et al.* 2001). While the active site of KIR2DL4 was kept the same as in other docking process.

HADDOCK clustered 187 structures in 8 clusters, representing 93.5 % of the water-refined models that HADDOCK generated. These structures were clustered by the program on the basis of HADDOCK score of the complexes. From these 8 clusters, top cluster with highest HADDOCK score was selected. Table no. 7 shows that the top cluster scores for different energies. HADDOCK score for the top cluster was -101.9 +/- 3.3. The cluster had 23 structures and the RMSD value from the lowest energy structure came out to be 1.1 +/- 0.7 Å. The statistic parameter Z score is also calculated for the cluster which indicates how many standard deviations from the average this cluster is located in terms of score, which was observed to be high (Z= -1.4). Table 7 shows the statistics of result obtained from HADDOCK docking protocol.

HADDOCK score	-101.9 +/- 3.3
Cluster size	23
RMSD from the overall lowest-energy structure	1.1 +/- 0.7
Van der Waals energy	-43.4 +/- 6.9
Electrostatic energy	-355.8 +/- 33.7
Desolvation energy	12.5 +/- 8.7
Restraints violation energy	1.3 +/- 0.67
Buried Surface Area	1583.3 +/- 111.6
Z-Score	-1.4

Table no. 7: Energy scores of top cluster generated by HADDOCK for HLA-Cw4-KIR2DL4 docking

Such a high score was expected from HLA-Cw4 because of its homology with HLa-Cw3. The score was comparable with HLA-Cw3. Table no. 8 shows the H bond forming residues of HLA-Cw4. The interaction pattern of KIR2DL4 with HLA-Cw3 was similar to KIR2DL4-HLA-Cw4. Asp56, Tyr113 and Asp143 of KIR2Dl4 were the conserved H-bond forming residues of KIR2DL4. Figure 10 highlights the H-bond forming residues of KIR2DL4 and HLA-Cw4.

S.No.	Residues of KIR2DL4	Residues of HLA-Cw4	H bond disatance (Å)
1.	Lys55	Glu89	1.6
2.	Asp 56	Arg75	1.6
3.	Ala82	Arg75	2.4
4.	Tyr113	Arg69	2.8
5.	Asp143	Asn80	2.0
6.	Asp143	Lys146	1.6
7.	Pro162	Arg145	2.3
8.	His190	Arg79	2.5
9.	Glu195	Gln72	1.9

Table no. 8: H bond forming residues of KIR2DL4 and HLA-Cw4

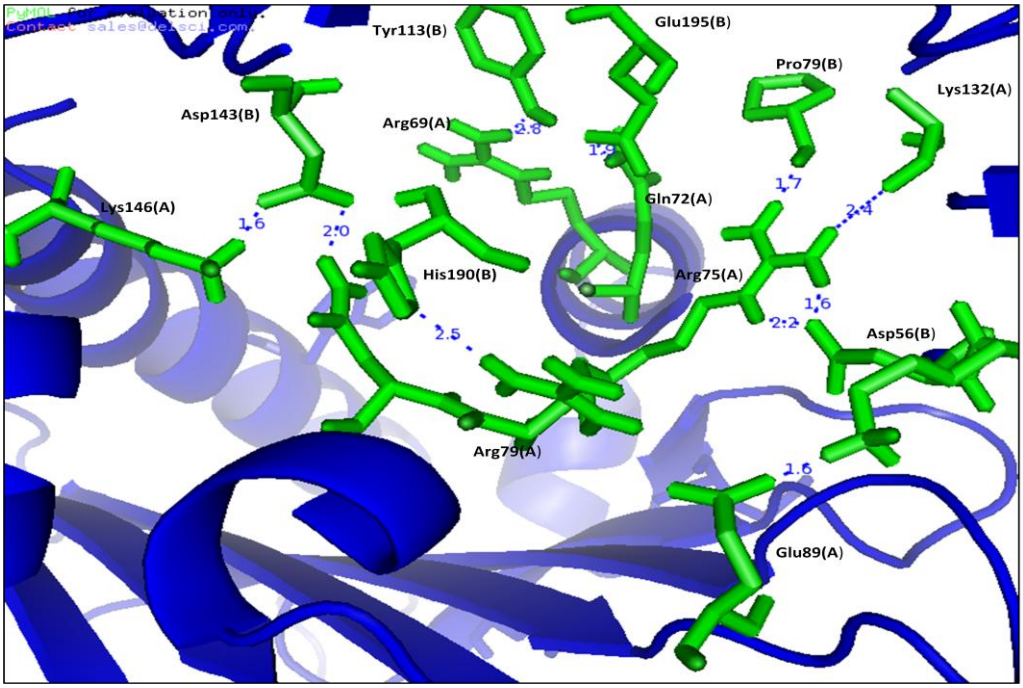

Figure 10: H-bond forming residues of KIR2DL4 and HLA-Cw4

The results were not surprising as HLA-Cw3 shares 93% similarity with HLA-Cw4.It was seen that some of the residues of HLA-Cw3 and HLA-Cw4 were common in KIR2DL4 interaction. Arg75, Arg79 and Glu89 remained conserved interacting residues in both HLA-Cw3 and HLA-Cw4.Such binding results shows that KIR2DL4 has some role to play in regulating the activity of NK cells against many immunological responses as HLA- C is involved in many processes like viral infection and tumor progression.

5. Conclusion

Evidences have shown HLA-G as a cognate ligand KIR2DL4 which plays a very prominent role in pregnancy; however the structural basis were not elucidated. The study presented a structural view of interacting residues for the pair of protein. Previous experiments defined Met76, Gly79 and Thr80 as key residues in KIR2DL4 interaction with HLA-G. The results presented have supported the claim computationally. Along with it the binding affinity of KIR2DL4 was compared with other class I molecules: HLA-E, HLA-Cw3 and HLA-Cw4. Present data shows a very little binding of KIR2DL4 to HLA-E as compared to HLA-G, which was also shown by experimental binding studies. The concurrent results of our bioinformatics approach with the experimental evidences, provides an unequivocal conformation to our strategy for elucidating KIR2DL4 binding with HLA ligands. Hence we use this protocol to study KIR2DL4 binding with HLA-C ligands also. In an attempt to find the binding affinity of KIR2DL4 with HLA-Cw3 and HLA-Cw4, a new structural insight was found as KIR2DL4 showed a greater binding affinity than HLA-G, the known binding ligand of KIR2DL4, with both these HLA molecules with certain conserved residues playing an important role in interactions. Hence KIR2DL4 has the probability of regulating NK activity against multiple immune responses especially against viral infection and tumor transformation. In case of various viral infection and tumor transformation, there is often a downregulation of HLA-C which results in modulation of NK activity. Hence, KIR2DL4 may play a role in modulation of NK activity.

Future Prospects

Inhibitory KIRs are known to bind HLA-A, HLA-B and HLA-C alleles, and also to non-classical MHC molecules like HLA-G (Rajagopalan and Long, 2012). Different classes of inhibitory receptors are present in each human NK cell. In-vitro studies have proved that the interaction between KIRs and non-classical MHC like HLA-E/G is stronger than classical MHC HLA-C (Das and Long, 20l0). Since, structural basis for this difference in NK activity has not yet been explored, in order to design better immunotherapeutic strategies for cancer treatment; we need to explore the structural basis of the different inhibitory receptor with their ligands and see how the expression level of receptors is altered in NK cells in different organs. NK cell employs analog signaling where a repertoire of inhibitory and activating receptors binds to their cognate ligands and the net outcome is a result of quantitative effect produced by binding of the ligands to these receptors. The co-expression of multitude of activating and inhibitory receptors on NK cells has made it difficult to identify ligands for certain NK receptors. Structural analysis of the domain or conserved regions possessed by the activating ligands and calculating their binding efficiency can be utilized for the prediction of unknown ligands/antigens expressed by tumor cells.

Activating receptors expressed on NK cell plays a very important role in triggering immunological response. Interaction between various activating receptors like NKG2-CD94, NKp44 and NKp30 and their ligands expressed on tumors has been known to contribute to cancer progression (Takayama *et al.*,2010; Zou *et al.*,2010; Rocca *et al.*, 2012). Structural information of the activating receptors and their cognate ligands is very limited (Seidal *et al.*, 2012). Further, putative tumor expressed ligands for activating NK receptors have not been investigated yet; which are potentially addressable by computational approaches and can further help to develop NK based cancer therapeutic strategies.

NK inhibitory receptor and non-classical MHC interaction has been shown to have better inhibition of NK cell cytotoxicity than with classical MHC molecule. The multifarious recognition pattern of classical and non-classical MHC proteins by NK receptors and every accessible surface involved in this binding event should be explored. The knowledge of affinity of NK cell receptor with MHC I ligands will help in understanding the binding patterns required for the inhibition of NK cell activity.

The studies on affinities of NK receptors with their cognate ligand can be correlated with the epidemiology of different types of cancers. Based on this knowledge new NK cell therapies can be devised.

References

A. B. Herr, E. R. Ballister, and P. J. Bjorkman (2003).Insights into IgA-mediated immune responses from the crystal structure of human Fc-alpha-RI and its complex with IgA1-Fc.Nature. 423 ,614–620.

A. E. Hamburger, A. P. West Jr., and P. J. Bjorkman (2004).Crystal structure of a polymeric immunoglobulin binding fragment of the human polymeric immunoglobulin receptor.Structure.12, 1925–1935.

A. Garg, P. F. Barnes, A. Porgador *et al*.(2006).Vimentin expressed on Mycobacterium tuberculosis-infected human monocytes is involved in binding to the NKp46 receptor, Journal of Immunology.177,6192–6198.

A. Moretta, C. Bottino, M. Vitale *et al.* (2001.).Activating receptors and coreceptors involved in human natural killer cellmediated cytolysis, Annual Review of Immunology.19, 197–223.

A. Zilka, G. Landau, O. Hershkovitz *et al*.(2005). Characterization of the heparin/heparan sulfate binding site of the natural cytotoxicity receptor NKp46, Biochemistry. 44, 14477–14485.

Andre´, P., R. Biassoni, M. Colonna, D. Cosman *et al.* (2001). New nomenclature for MHC receptors. Nat. Immun. 2,661-72

B. E. Willcox, L. M. Thomas, and P. J. Bjorkman(2003). Crystal structure of HLA-A2 bound to LIR-1, a host and viral major histocompatibility complex receptor. Nature Immunology.4, 913–919.

B.R. Jefferys, L.A. Kelley, M.J. Sternberg. (2010). Protein folding requires crowd control in a simulated cell, J. Mol. Biol. 397, 1329–1338.

Berman H.M., Westbrook J., Feng Z., Gilliland G. *et al.* (2000).The Protein Data Bank , Nucleic Acids Res.28,235–242.

Boyington JC, Motyka SA, Schuck P, Brooks AG, Sun PD.(2000). Crystal structure of an NK cell immunoglobulin-like receptor in complex with its class I MHC ligand, Nature. 6786,537-43.

Boyson, J.E., Erskine,R., Whitman, M. C.,*et al.* (2002). Disulfidebond-mediated dimerization of HLA-Gonthecell surface. Proc.Natl.Acad.Sci.U.S.A. 99, 16180–16185.

C. Cantoni, C. Bottino, M. Vitale *et al*. (1999).NKp44, a triggering receptor involved in tumor cell lysis by activated human natural killer cells, is a novel member of the immunoglobulin Superfamily. Journal of Experimental Medicine.189,787–795.

C. Cantoni, M. Ponassi, R. Biassoni *et al.(*2003).The threedimensional structure of the human NK cell receptor NKp44, a triggering partner in natural cytotoxicity. Structure. 11, 725–734,

Foster C. E., Colonna M., and Sun P. D.(2003).Crystal structure of the human natural killer (NK) cell activating receptor NKp46 reveals structural relationship to other leukocyte receptor complex immunoreceptors. The Journal of Biological Chemistry.278, 46081–46086.

Fuller C. L., Ruthel G., Warfield K. L. *et al*.(2007).NKp30-dependent cytolysis of filovirus-infected human dendritic cells. Cellular Microbiology. 9, 962–976.

Cantoni C, Ponassi M, Biassoni R, *et al.*(2009).The three-dimensional structure of the human NK cell receptor NKp44, a triggering partner in natural cytotoxicity. Structure. 6, 725-34.

Cantoni, C., S. Verdiani, M. Falco, A. Pessino, *et al.*(1998). p49, a putative HLA class I-specific inhibitory NK receptor belonging to the immunoglobulin superfamily. Eur. J. Immunol. 28, 1980-92.

Carosella, E. D., P. Paul, P. Moreau, and N. Rouas-Freiss. (2000). HLA-G and HLA-E: fundamental and pathophysiological aspects. Immunol. Today 21:532-42.

Carretero M, Palmieri G, Llano M, Tullio V *et al.*(1998).Specific engagement of the CD94/NKG2-A killer inhibitory receptor by the HLA-E class Ib molecule induces SHP-1 phosphatase recruitment to tyrosinephosphorylated NKG2-A: evidence for receptor function in heterologous transfectants. Eur J Immunol, 28, 1280-91

Clements, C.S., Kjer-Nielsen, L., KosteNKo, L., Hoare *et al.*(2010).Crystal structure of HLA-G: a nonclassical MHC class I molecule expressed at the fetal-maternal interface. Proc Natl Acad Sci U S A. 102, 3360-3365

Crisa, L., M. T. McMaster, J. K. Ishii, S. J. Fisher, and D. R. Salomon.(1997).Identification of a thymic epithelial cell subset sharing expression of the class Ib HLA-G molecule with fetal trophoblasts. J. Exp. Med. 186,289-98.

Pende D., Parolini S., Pessino A. *et al.(*1999).Identification and molecular characterization of NKp30, a novel triggering receptor involved in natural cytotoxicity mediated by human natural killer cells.Journal of Experimental Medicine.190, 1505–1516.

Dominguez C, Boelens R, Bonvin AM. (2003). HADDOCK: A protein-protein docking approach based on biochemical or biophysical information, J Am Chem Soc. 7,1731–1737.

E. Cagnano, O. Hershkovitz, A. Zilka *et al.* (2008)Expression of ligands to NKp46 in benign and malignant melanocytes. Journal of Investigative Dermatology. 128, 972–979.

Fan QR, Long EO, Wiley DC (2001). Crystal structure of the human natural killer cell inhibitory receptor KIR2DL1-HLA-Cw4 complex. Nat Immunol. 5, 452-60.

Fleury D, Wharton SA, Skehel JJ, *et al.*(1998). T- Antigen distortion allows influenza virus to escape neutralization. Nat Struct Biol.2,119-23.

Foster CE, Colonna M, Sun PD.(2003).Crystal structure of the human natural killer (NK) cell activating receptor NKp46 reveals structural relationship to other leukocyte receptor complex immunoreceptors. J Biol Chem. 46,46081-6

Kaminski G. A., Friesner R. A., Tirado-Rives J., *et al.*(2001) J. Phys. Chem. B 28, 6474-6487.

Ferlazzo G., Tsang M. L., Moretta L., Melioli G., *et al.*(2002).Human dendritic cells activate resting natural killer (NK) cells and are recognized via the NKp30 receptor by activated NK cells," Journal of Experimental Medicine. 195, 343–35.

Guex, N. and Peitsch, M.C. (1997). SWISS-MODEL and the Swiss-PdbViewer: An environment for comparative protein modeling. Electrophoresis. 18, 2714-2723.

Guo, Z., Mohanty, U., Noehre, J., Sawyer, T.K., Sherman, W., & Krilov G, (2010).Probing the alpha-helical structural stability of stapled p53 peptides: Molecular dynamics simulations and analysis. Chem Biol Drug Des.4,348-59

Houlihan JM, Biro PA, Harper HM, JeNKinson HJ, Holmes CH (1995). The human amnion is a site of MHC class Ib expression: evidence for the expression of HLA-E and HLA-G. J Immunol 154, 5665-74.

Marquez J. A., Galfre E., Dupeux F., Flot D., Moran O., and Dimasi N. (, 2007).The crystal structure of the extracellular domain of the inhibitor receptor expressed on myeloid cells IREM-1. Journal of Molecular Biology. 367, 310–318.

Marquez J. A., Galfre E., Dupeux F., Flot D., Moran O., and Dimasi N. (2007).The crystal structure of the extracellular domain of the inhibitor receptor expressed on myeloid cells IREM-1. Journal of Molecular Biology . 36, 310–318,

Gattis J. L., Washington A. V.,. Chisholm M. M *et al.*(2006), "The structure of the extracellular domain of triggering receptor expressed on myeloid cells like transcript-1 and evidence for a naturally occurring soluble fragment. Journal of Biological Chemistry. 281, 13396–13403.

Soding J., Protein homology detection by HMM–HMM comparison.(2005). Bioinformatics. 21, 951–960.

Jiang Q, Pan HY, Ye DX, Zhang P, Zhong LP, Zhang ZY(2010).Downregulation of tapasin expression in primary human oral squamous cell carcinoma: association with clinical outcome. Tumour Biol. 5,451-9

Jorgensen, W.L., Maxwell, D.S., & Tirado Rives, J.,(1996). Development and testing of the OPLS all-atom force field on conformational energetics and properties of organic liquids. J. Am. Chem. Soc. 45, 11225–11236.

Horii K., Kahn M. L., and Herr A. B. (2006.) .Structural basis for platelet collagen responses by the immune-type receptor glycoprotein VI.Blood. 108, 936–942.

Kaiser BK, Pizarro JC, Kerns J, Strong RK (2008). Structural basis for NKG2A/CD94 recognition of HLA-E , (2008), Proc Natl Acad Sci U S A.18,6696-701.

Kaminski, G.A., Friesner, R.A., Tirado-Rives, J., & Jorgensen, W.L.(2001). Evaluation and re-parameterization of the OPLS-AA force field for proteins via comparison with accurate quantum chemical calculations on peptides. J. Phys. Chem. *B.* 28, 6474–6487

Kovats, S., E. K. Main, C. Librach, M. Stubblebine, S. J. Fisher, and R. DeMars (1990). A class I antigen, HLA-G, expressed in human trophoblasts. Science. 248, 220-43.

Le Bouteiller P, Solier C.(2001). Is antigen presentation the primary function of HLA-G? Microbes Infect. 3,323-32.

Li, Y., Wang, Q., Mariuzza, R.A (2003). Structure of the activating natural killer receptor NKp30 bound to its ligand B7-H6 reveals basis for tumor cell recognition in humans.

Long,E.O.,and Rajagopalan,S. (2000).HLA class I recognition by killer cell Ig-like receptors. Semin.Immunol. 12, 101–108.

Jarahian M., Watzl C., Fournier P. *et al.*(2009).Activation of natural killer cells by newcastle disease virus hemagglutininneuraminidase. Journal of Virology. 83, 8108–8121.

Hecht M. L., Rosental B., Horlacher T. *et al.*(2009).Natural cytotoxicity receptors NKp30, NKp44 and NKp46 bind to different heparan sulfate/heparin sequences. Journal of Proteome Research.8, 712–720.

Ponassi M., Cantoni C., Biassoni R. *et al.*(2003).Structure of the human NK cell triggering receptor NKp46 ectodomain. Biochemical and Biophysical Research Communications. 309, 317–323.

Kelker M. S., Debler E. W., and. Wilson I. A (2004) Crystal structure of mouse triggering receptor expressed on myeloid cells 1 (TREM-1) at 1.76 A. Journal of Molecular Biology. 344, 1175–1181.

Vitale M., Bottino C., Sivori S. *et al.*(1998).NKp44, a novel triggering surface molecule specifically expressed by activated natural killer cells, is involved in non-major histocompatibility complex-restricted tumor cell lysis. Journal of Experimental Medicine .187, 2065–2072.

Moreau, P., F. Adrian-Cabestre, C. Menier, V. Guiard, L. Gourand, J. Dausset, E. D. Carosella, and P. Paul. 1999. IL-10 selectively induces HLA-G expression in human trophoblasts and monocytes. Int. Immunol. 11, 803-14.

Morris AL, MacArthur MW, Hutchinson EG, Thornton JM (1992). Stereochemical quality of protein structure coordinates. Proteins. 12, 345-364.

Zaccai N. R., May A. P., Robinson R. C. *et al.*(2007)Crystallographic and in silico analysis of the sialoside-binding characteristics of the Siglec sialoadhesin. Journal of Molecular Biology.365,1469–1479.

Mandelboim O., Lieberman N., Lev M. *et al.*(2001).Recognition of haemagglutinins on virus-infected cells by NKp46 activates lysis by human NK cells. Nature. 409,1055–1060

Ponte, M., C. Cantoni, R. Biassoni, A. Tradori-Cappai, *et al.*(1999). Inhibitory receptors sensing HLA-G1 molecules in pregnancy: decidua-associated natural killer cells express LIR-1 and CD94/NKG2A and acquire p49, an HLA-G1-specific receptor. Proc. Natl. Acad. Sci. USA 96,5674-87.

Proll J, Bensussan A, Goffin F, *et al.* (2000) Tubal versus uterine placentation: similar HLA-G expression extravillous cytotrophoblast invasion but different maternal leukocyte recruitment. Tissue Antigens .56,479-91.

Castriconi R., Dondero A., Negri F. *et al.*(2007).Both CD133+ and CD133- medulloblastoma cell lines express ligands for triggering NK receptors and are susceptible to NK-mediated Cytotoxicity.European Journal of Immunology.37, 3190–3196

Luthy R., Bowie J.U., Eisenberg D..(1992). Assessment of protein models with three dimensional profiles, Nature 356 , 83–85.

Rajagopalan, S., and E. O. Long. 1999. A human histocompatibility leukocyte antigen (HLA)-G-specific receptor expressed on all natural killer cells .J. Exp. Med. 189, 1093-108.

Rajagopalan, S., J. Fu, and E. O. Long. 2001. Cutting edge: induction of IFN- production but not cytotoxicity by the killer cell Ig-like receptor KIR2DL4 (CD158d) in resting NK cells. J. Immunol. 167,1877-90

Rajagopalan, S.,and Long,E.O.(1999). A human histocompatibility leukocyte antigen(HLA)-G-specific receptor expressed on all natural killer cells. J. Exp.Med. 189, 1093–1100.
Rajagopalan, S.,and Long,E.O.(2006). KIR2DL4 (CD158d):anactivationreceptorforHLA-G. Frontier in Immunology.3, article 258.

Rajagopalan,S., Bryceson,Y.T., Kup-pusamy,S.P., Geraghty,D.E., van derMeer, A.,Joosten, I.,and Long,E.O.(2006).Activation of NK cells by an endocytosed receptor for soluble HLA-G. PLoSBiol. 4, e9.

Rizzo,R., Vercammen, M.,vandeVelde, H., Horn, P.A., and Rebmann,V. (2010). The importance of HLA-G expression in embryos, trophoblast cells, and embryonic stem cells. Cell. Mol.LifeSci. 68, 341–352.

Rouas-Freiss, N., Goncalves, R.M., Menier, C., Dausset, J., and Carosella, E.D. (1997). Direct evidence to support the role of HLA-G in protecting the fetus from maternal uterine natural killer cytolysis. Proc Natl Acad Sci U S A .94, 11520-11525

Chisholm S. E. and Reyburn H. T. (2006)Recognition of vaccinia virus-infected cells by human natural killer cells depends on natural cytotoxicity receptors," Journal of Virology.80, 2225–2233

Chisholm S. E., Howard K.,. Gomez M. V, and. Reyburn H. T (2007).Expression of ICP0 is sufficient to trigger natural killer cell recognition of herpes simplex virus-infected cells by natural cytotoxicity receptors.Journal of Infectious Diseases. 195, 1160–1168.

Esin S., Batoni G., Counoupas C. *et al.(*2008)Direct binding of human NK cell natural cytotoxicity receptor NKp44 to the surfaces of mycobacteria and other bacteria. Infection and Immunity.76, 1719–1727.

Radaev S., Kattah M., Rostro B., Colonna M., and Sun P. D..(2003).Crystal structure of the human myeloid cell activating receptor TREM-1," Structure. 11, 1527–1535,

Sivori S., Vitale M., Morelli L. *et al.* (1997).p46, a novel natural killer cell-specific surface molecule that mediates cell activation.Journal of Experimental Medicine. 7, 1129–1136.

Selvakumar, A., U. Steffens, and B. Dupont. (1996). NK cell receptor gene of the KIR family with two Ig domains but highest homology to KIR receptors with three Ig domains. Tissue Antigens. 48 ,285-294.

Sharkey AM, Gardner L, Hiby S, *et al.(*2008). Killer Ig-like receptor expression in uterine NK cells is biased toward recognition of HLA-C and alters with gestational age. J Immunol.181,39–46.

Sjoerd J. de Vries, Aalt D. J. van Dijk, Mickaël Krzeminski, *et al.*(2007) , HADDOCK versus HADDOCK: New features and performance of HADDOCK2.0 on the CAPRI targets. Proteins: Structure, Function, and Bioinformatics. 69, 726–733.

Stephanie C. Ganal, Stephanie L. Sanos Carsten Kallfass, *et al.* (2012).Priming of Natural Killer Cells by Nonmucosal Mononuclear Phagocytes Requires Instructive SignalS from Commensal Microbiota. Immunity. 37, 171–186.

Arnon T. I., Lev M., Katz G., Chernobrov Y., A. Porgador, and O. Mandelboim(2001).Recognition of viral hemagglutinins by NKp44 but not by NKp30. European Journal of Immunology.31,2680–2689.

Trowsdale J, Moffett A. (2008) NK receptor interactions with MHC class I molecules in pregnancy. Semin Immunol. 20, 317–20.

Yutkin V., Pode D., Pikarsky E., and Mandelboim O. (2007).The expression level of ligands for natural killer cell receptors predicts response to bacillus Calmette-Guerin therapy: a pilot Study. Journal of Urology. 178, 2660–2664.

Valiante, N. M., M. Uhrberg, H. G. Shilling, K. Lienert-Weidenbach, K. L. Arnett, A. D'Andrea, J. H. Phillips, L. L. Lanier, and P. Parham. (1997). Functionally and structurally distinct NK cell receptor repertoires in the peripheral blood of two human donors. Immunity 7,739-50.

van Dijk A.D., de Vries S.J., Dominguez C., *et al.*(2005), Data-driven docking: HADDOCK's adventures in CAPRI. Proteins, Proteins. 60, 232–238.

Jorgensen W. L., Maxwell D. S., and Tirado-Rives J. (1996) J. Am. Chem. Soc. 45, 11225-11236.

Van Gunsteren W. F., Billeter S. R.,. Eising A. A, *et al.*(1996). Biomolecular Simulation*:* The GROMOS96 Manual and User Guide, 1-1042.

El-Sherbiny Y. M., Meade J. L., Holmes T. D. *et al.* (2007).The requirement for DNAM-1, NKG2D, and NKp46 in the natural killer cell-mediated killing of myeloma cells. Cancer Research.67, 8444–8449

Yan WH, Fan LA, (2005).Residues Met76 and Gln79 in HLA-G alpha1 domain involve in KIR2DL4 recognition. Cell Res. 3,176-82

Yang, Y., W. Chu, D. E. Geraghty, and J. S. Hunt. (1996). Expression of HLA-G in human mononuclear phagocytes and selective induction by IFN-. J. Immunol. 156, 4224-32.